for proteasome subunits. Western blot analysis revealed that expression of the subunits of 20S proteasomes (components of the α and β rings) was more strongly induced by denervation in the soleus muscles of control mice than it was by denervation in the soleus muscles of *Atg7* KO and *Park2* KO mice (**Fig. 4A and D**). The mRNA levels for 20S proteasome subunits in the denervated soleus muscles from control mice were significantly higher than those in the denervated soleus muscles from *Atg7* KO and *Park2* KO mice (**Fig. 4E**). These results indicate that the deficiency of PARK2-mediated mitophagy suppresses denervation-induced transcription of 20S proteasome subunit mRNA as well as the de novo synthesis of proteasomes in soleus muscles. Interestingly, denervation induced the expression of proteasome subunits in the plantaris muscle of all genotypes examined (**Fig. S4A**). Therefore, denervated plantaris muscles of *Atg7* KO mice atrophied to almost the same extent seen in denervated plantaris muscles of control mice (**Fig. S1A**).

Accumulation of damaged mitochondria suppresses NFE2L1 transcriptional activity

Nuclear factor erythroid-derived 2-related factors (Nrfs; NFE2L1/Nrf1/TCF11/LCRF1 and NFE2L2/Nrf2), cap'n'collar-type basic leucine zipper (CNC-bZip) protein family members, have been reported to regulate the transcription of proteasome subunits.[30-33] Nrfs bind to the antioxidant response element (ARE) in the promoters of its target genes.[34] The promoters of all mammalian proteasome subunits contain ARE or ARE-like sequences.[32] To ascertain whether there were any differences in the Nrfs levels of the soleus muscles of control and *Atg7* or *Park2* KO mice, we examined Nrfs levels in tissue lysates and the nuclear extracts of soleus muscles by western blotting analysis (**Fig. 4F**). Denervation elevated total NFE2L1 levels in the soleus muscles of all genotypes examined, whereas, the NFE2L1 level was high in the nuclear extracts of soleus muscles of denervated control mice, but very low in those of the innervated control and denervated *Atg7* or *Park2* KO mice. In contrast, little NFE2L2 was detected in total lysate and nuclear extracts from soleus muscles. However, denervation did not influence the NFE2L1 levels in tissue lysates, and decreased nuclear NFE2L1 levels in the plantaris muscles of all genotypes examined (**Fig. S4C**). Although total NFE2L2 levels in plantaris muscles were comparable to those in soleus muscles, denervation elevated the NFE2L2 level in nuclear extracts of the plantaris muscles of all genotypes examined. These results indicate that 2 different Nrfs, NFE2L1 and NFE2L2, are involved in the denervation-induced expression of proteasome subunits in slow-twitch soleus muscle and fast-twitch plantaris muscle, respectively.

To confirm that the accumulation of damaged (or uncoupled) mitochondria in the soleus muscles of denervated *Atg7* KO or *Park2* KO mice affects NFE2L1 nuclear translocation, we treated C2C12 cells, a murine myoblast cell line, with the mitochondrial uncoupler carbonyl cyanide m-chlorophenylhydrazone (CCCP) to induce a mimetic condition of damaged mitochondria accumulation, and examined its effect on NFE2L1 transcriptional activity. As previously reported, incubation with several drugs, including proteasome inhibitors (MG-132), tunicamycin and tert-butyl hydroquinone (tBHQ), promotes mRNA expression of proteasome subunits (especially 20S proteasome components)[32,33,35,36] (**Fig. 5A**), and the expression of the 20S proteasome subunits induced by those drugs was suppressed by the addition of CCCP. In addition, siRNA knockdown of *Nfe2l1* significantly suppressed MG-132-induced proteasome subunit expression (**Fig. 5B**) Moreover, MG-132-induced NFE2L1 nuclear translocation was also suppressed by the addition of CCCP in C2C12 and HeLa cells (**Fig. 5C and D**; **Fig. S5C**). In addition, the effects of CCCP on MG-132-induced NFE2L1 nuclear translocation and NFE2L1 target-gene expression were blocked by the addition of N-acetyl-cysteine (NAC), an antioxidant. These results indicate that 24 h CCCP treatment induces ROS production from mitochondria in addition to the mitochondrial depolarization. To confirm the effect of ROS on NFE2L1 nuclear translocation, we tested the effects of rotenone, a complex I inhibitor, antimycin, a complex III inhibitor, and H_2O_2 on nuclear levels of NFE2L1 (**Fig. S5A and S5B**). As expected, the addition of rotenone, antimycin or H_2O_2 suppressed the MG-132-induced NFE2L1 nuclear translocation, and the effects of those drugs were invalidated by the addition of NAC. Together, these results indicate that the accumulation of damaged mitochondria producing ROS negatively affects NFE2L1 translocation and the transcription of NFE2L1 target genes.

Discussion

Mitochondria have been postulated to play an important role in triggering signals that contribute to muscle atrophy.[37] In this study, we noticed that a similar pattern of mitochondrial dysfunction and soleus muscle atrophy in denervated autophagy-deficient and *Park2*-deficient mice, and showed the evidence for PARK2-mediated mitophagy playing the important roles in slow-twitch muscle atrophy, which is the first report showing the physiological role of the PARK2-mediated mitophagy in mammalian in vivo model. The accumulation of damaged mitochondria in the PARK2-mediated mitophagy deficient soleus muscle, interferes the expression of proteasome subunits (**Fig. S6**). The elevation of proteasome expression is the key event in the early stage of slow-twitch muscle atrophy, and that it is regulated by a transcription factor NFE2L1. Under nonstress conditions, NFE2L1 is targeted by its N-terminal putative transmembrane domain to the endoplasmic reticulum (ER) membrane, where it is quickly degraded via ER-associated degradation (ERAD).[33,35,38] In response to proteasome inhibition, NFE2L1 translocates from the ER to the nucleus, where it transactivates the transcription of target genes including proteasome subunits. Conversely, NFE2L2, another Nrfs, is constitutively degraded by proteasome because its binding partner KEAP1 (kelch-like ECH-associated protein 1) is a component of the ubiquitin ligase complex in standard conditions.[39-42] The oxidative and electrophilic stresses inactivate KEAP1 by the modification of its cysteine residues, and stabilize NFE2L2 to induce the transcription of numerous cytoprotective genes.[43-45] In this study, we showed that NFE2L1 nuclear translocation is interfered by oxidative stress, which activates NFE2L2 activity. Therefore, the PARK2-mediated

mitochondrial quality control system plays an important role in NFE2L1-dependent slow-twitch muscle atrophy, because of interference in the NFE2L1 system by oxidative stress. Furthermore, fast-twitch plantaris muscles atrophied to the same extent by denervation in the presence and the absence of PARK2-mediated mitophagy, express lower levels of PARK2 and NFE2L1 than slow-twitch muscles during denervation atrophy. Therefore, we speculate that tissues regulated by the NFE2L1 system express more PARK2 to eliminate damaged mitochondria than do other tissues. Our findings highlight the linkage between mitochondria autophagy and the UPS, 2 major intracellular protein degradation systems, and their different roles in slow-twitch skeletal muscle atrophy.

Materials and Methods

Antibodies and reagents

Anti-ATG7 antibodies were described previously.[14] Anti-PARK2 (Parkin, 4211), anti-PDHA1 (pyruvate dehydrogenase, 3205), anti-PSMD4 (Rpn10/S5a, 3846), anti-GAPDH (2118), anti-TRP53 (p53, 2524), anti-NFE2L1 (TCF11/Nrf1, 8052), anti-BCL2 (Bcl-2, 2870) and anti-BCL2L1 (Bcl-xL, 2764) antibodies were obtained from Cell Signaling Technology. Anti-PSMA5 (Proteasome 20S α5 subunit, BML-PW8125), anti-PSMB7 (Proteasome 20S β2 subunit, BML-PW9300) and anti-PSMC6 (Proteasome 19S Rpt4 subunit, BML-PW8830) were obtained from Enzo Life Sciences. Anti-OPA1 (612606) and anti-DNM1L (Drp1, 611112) were obtained from BD transduction laboratories. Anti-SQSTM1 (GP62-C) was obtained from Progen. Anti-MYH7(myosin heavy chain I, Clone NOQ7.5.4D, M8421) was obtained from Sigma-Aldrich. Anti-multi ubiquitin (Clone FK2, D058-3) was obtained from MBL. Anti-PPARGC1A (PGC-1, AB3242) was obtained from Millipore. MitoProfile Total OXPHOS Rodent WB Antibody Cocktail (MS604) was obtained from MitoSciences. Anti-TOMM20 (Tom20, sc-11415), anti-CYCS (Cytochrome *c*, sc-13156), anti-NFE2L1 (Nrf1, H-285, sc-13031, for immunostaining of HeLa cells), anti-NFE2L2 (Nrf2, H-300, sc-13032) and anti-LMNB (Lamin B, sc-6216) were obtained from Santa Cruz Biotechnology. Anti-DMD (Dystrophin, ab15277) and anti-MUL1 (ab84067) were obtained from Abcam. Anti-MFN1 (H00055669-M04) was obtained from Abnova. Anti-FIS1 (10956-1-AP) was obtained from Proteintech. Anti-8-OHdG (MOG-020P) was obtained from the Japan Institute for the Control of Aging, NIKKEN SEIL Co, Ltd. The Protein Carbonyls Western Blot Detection Kit was obtained from SHIMA Laboratories. Alexa 488- and Alexa 594-conjugated secondary antibodies (A11034, A11029, A11037, A11032) were obtained from Molecular Probes. The M.O.M. Immunodetection kit and Texas Red Avidin DCS were obtained from VECTOR Laboratories. Tunicamycin (T7765), tBHQ (112941), CCCP (C-2759), rotenone (R-8875), antimycin (A-8674) and N-acetyl-cysteine (A9165) were obtained from Sigma-Aldrich. MG-132 (474790) was obtained from CALBIOCHEM. Succinyl-Leu-Leu-Val-Tyr-7-amido-4-methylcoumarin (Suc-LLVY-MCA, 3120-v) and epoxomicin (4381-v) were obtained from Peptide Institute, Inc.

Animals

HSA-Cre-ER^{T2} transgenic mice were a gift from Dr Pierre Chambon. To produce *Atg7*$^{Flox/Flox}$: HSA-ER^{T2}-Cre mice, *Atg7*$^{Flox/Flox}$ mice were bred with HSA-Cre-ER^{T2} transgenic mice. To delete the floxed *Atg7* gene from skeletal muscle, Cre-ER^{T2} recombinase activity was induced in 4-wk-old mice by i.p. injections of 1 mg tamoxifen for 5 consecutive days. GFP-LC3 transgenic and *Park2* knockout mice have been previously described. All mice were maintained in an environmentally controlled room (lights on from 8:00 to 20:00) and were fed a pelleted laboratory diet and tap water ad libitum, unless otherwise stated. Denervation was performed at 4 wk after tamoxifen injections. To standardize autophagic activity in the skeletal muscles, mice were fasted for 24 h before euthanasia. Experimental protocols were approved by the Ethics Review Committee for Animal Experimentation of Juntendo University.

Histological analysis and electron microscopy

Cryosections, 10 μm thick, from mouse hind limbs were stained with hematoxylin and eosin (H&E), stained for succinate dehydrogenase (SDH) or cytochrome *c* oxidase (COX) activities, or immunolabeled with anti-PARK2, anti-TOMM20, anti-myosin heavy chain I (MYH7), anti-DMD and anti-8-OHdG antibodies. To quantify the SDH or COX activities of soleus muscles, Image J software was used. For EM analysis, soleus muscles were directly fixed with 2% glutaraldehyde in 0.1 M cacodylate buffer on ice. Embedding, sectioning and microphotography were performed by the Hanaichi Electron Microscopic Laboratory, Inc.

Cell culture and siRNA transfection

C2C12 cells and HeLa cells were maintained in DMEM supplemented 10% fetal calf serum and antibiotics. For RNA interference experiments, ON-TARGETplus mouse *Nfe2l1* siRNA (Thermo Scientific Dharmacon, L-062252-01-0005) or nontargeting controls (Thermo Scientific Dharmacon, D-001810-01-05) were transfected into C2C12 cells using Lipofectamine RNAiMAX reagent according to the manufacturer's protocols (Invitrogen, 13778075).

Isolation of mitochondrial fractions and nuclear extracts

Mitochondrial fractions of soleus muscles were isolated using the Mitochondria Isolation Kit for Tissue (Pierce, 89801), and nuclear extracts of soleus muscles or C2C12 cells were prepared using NE-PER Nuclear and Cytoplasmic Extraction Reagents (Pierce, 78833) according to the manufacturer's protocols.

Western blotting

For tissue lysate preparation, mouse skeletal muscles were homogenized in 10 volumes of 50 mM TRIS-HCl (pH 7.4) containing 0.15 M NaCl, 1 mM EDTA, 1% Triton X-100, 0.5% sodium deoxycholate, 0.1% SDS, a protease inhibitor cocktail (Roche Diagnostics, 11836170001), and a phosphatase inhibitor cocktail (Roche Diagnostics, 04906837001), using a motor-driven homogenizer (As One, S-203). For C2C12 cell lysate preparation, cells were lysed with the same buffer. The lysates were centrifuged at 12,000 × *g* for 10 min at 4 °C to remove debris. The supernatants, mitochondrial fractions, or nuclear extracts were analyzed by western blotting. Densitometric analysis was performed using ImageJ software.

Quantitative real-time PCR analysis

RNA was isolated using TRIzol reagent (Invitrogen, 15596026). cDNA was prepared using the Superscript III first strand synthesis kit (Invitrogen, 18080-044) according to the manufacturer's protocol. For mtDNA copy number quantification, genomic DNA was prepared. Quantitative real-time PCR was performed using the Fast SYBR Green Master Mix (Applied Biosystems, 4385612). The primers used for gene expression analysis are listed in **Table S1** and those used for mtDNA copy number analysis are listed in **Table S2**.

Measurement of proteasomal activity

Proteasome activities in soleus muscle extracts were measured using a fluorescent substrate, Suc-LLVY-MCA, as described previously.[46]

Statistics

All data are expressed as means ± s.d. Differences between groups were examined for statistical significance using one-way ANOVA, followed by Tukey-Kramer post hoc test or Student *t* test. A P value < 0.05 was considered statistically significant.

Disclosure of Potential Conflicts of Interest

No potential conflicts of interest were disclosed.

Acknowledgments

We thank Drs Pierre Chambon and Noboru Mizushima for providing the HSA-Cre-ER^{T2} transgenic and GFP-LC3 transgenic mice, respectively. This work was supported in part by a Grant-in-Aid for Young Scientists (B) (22700656 to NF), a Grant-in-Aid for Scientific Research (C) (24500868 to NF), a Grant-in-Aid for Scientific Research on Priority Areas (18076005 to MK, TU), a Grant-in-Aid for Scientific Research on Innovative Areas (23111003 (NH), a Grant-in-Aid for the "High-Tech Research Center" Project for Private Universities, a matching fund subsidy (SI, NF, TU, and EK) from the Ministry of Education, Culture, Sports, Science and Technology (MEXT) of Japan, the MEXT-Supported Program for the Scientific Research Foundation at Private Universities, 2011–2012 (NF), a Research Grant from the Takeda Science Foundation (TU) and an Intramural Research Grant (23-5) for Neurological and Psychiatric Disorders of NCNP (EA-H).

Supplemental Materials

Supplemental materials may be found here:
www.landesbioscience.com/journals/autophagy/article/27785

References

1. Jackman RW, Kandarian SC. The molecular basis of skeletal muscle atrophy. Am J Physiol Cell Physiol 2004; 287:C834-43; PMID:15355854; http://dx.doi.org/10.1152/ajpcell.00579.2003
2. Lecker SH, Solomon V, Mitch WE, Goldberg AL. Muscle protein breakdown and the critical role of the ubiquitin-proteasome pathway in normal and disease states. J Nutr 1999; 129(Suppl):227S-37S; PMID:9915905
3. Mammucari C, Milan G, Romanello V, Masiero E, Rudolf R, Del Piccolo P, Burden SJ, Di Lisi R, Sandri C, Zhao J, et al. FoxO3 controls autophagy in skeletal muscle in vivo. Cell Metab 2007; 6:458-71; PMID:18054315; http://dx.doi.org/10.1016/j.cmet.2007.11.001
4. Masiero E, Agatea L, Mammucari C, Blaauw B, Loro E, Komatsu M, Metzger D, Reggiani C, Schiaffino S, Sandri M. Autophagy is required to maintain muscle mass. Cell Metab 2009; 10:507-15; PMID:19945408; http://dx.doi.org/10.1016/j.cmet.2009.10.008
5. Sandri M, Sandri C, Gilbert A, Skurk C, Calabria E, Picard A, Walsh K, Schiaffino S, Lecker SH, Goldberg AL. Foxo transcription factors induce the atrophy-related ubiquitin ligase atrogin-1 and cause skeletal muscle atrophy. Cell 2004; 117:399-412; PMID:15109499; http://dx.doi.org/10.1016/S0092-8674(04)00400-3
6. Zhao J, Brault JJ, Schild A, Cao P, Sandri M, Schiaffino S, Lecker SH, Goldberg AL. FoxO3 coordinately activates protein degradation by the autophagic/lysosomal and proteasomal pathways in atrophying muscle cells. Cell Metab 2007; 6:472-83; PMID:18054316; http://dx.doi.org/10.1016/j.cmet.2007.11.004
7. Ravid T, Hochstrasser M. Diversity of degradation signals in the ubiquitin-proteasome system. Nat Rev Mol Cell Biol 2008; 9:679-90; PMID:18698327; http://dx.doi.org/10.1038/nrm2468
8. Schwartz AL, Ciechanover A. Targeting proteins for destruction by the ubiquitin system: implications for human pathobiology. Annu Rev Pharmacol Toxicol 2009; 49:73-96; PMID:18834306; http://dx.doi.org/10.1146/annurev.pharmtox.051208.165340
9. Mizushima N, Levine B. Autophagy in mammalian development and differentiation. Nat Cell Biol 2010; 12:823-30; PMID:20811354; http://dx.doi.org/10.1038/ncb0910-823
10. Yang Z, Klionsky DJ. Eaten alive: a history of macroautophagy. Nat Cell Biol 2010; 12:814-22; PMID:20811353; http://dx.doi.org/10.1038/ncb0910-814
11. Mizushima N, Yamamoto A, Matsui M, Yoshimori T, Ohsumi Y. In vivo analysis of autophagy in response to nutrient starvation using transgenic mice expressing a fluorescent autophagosome marker. Mol Biol Cell 2004; 15:1101-11; PMID:14699058; http://dx.doi.org/10.1091/mbc.E03-09-0704
12. Quy PN, Kuma A, Pierre P, Mizushima N. Proteasome-dependent activation of mammalian target of rapamycin complex 1 (mTORC1) is essential for autophagy suppression and muscle remodeling following denervation. J Biol Chem 2013; 288:1125-34; PMID:23209294; http://dx.doi.org/10.1074/jbc.M112.399949
13. Hara T, Nakamura K, Matsui M, Yamamoto A, Nakahara Y, Suzuki-Migishima R, Yokoyama M, Mishima K, Saito I, Okano H, et al. Suppression of basal autophagy in neural cells causes neurodegenerative disease in mice. Nature 2006; 441:885-9; PMID:16625204; http://dx.doi.org/10.1038/nature04724
14. Komatsu M, Waguri S, Chiba T, Murata S, Iwata J, Tanida I, Ueno T, Koike M, Uchiyama Y, Kominami E, et al. Loss of autophagy in the central nervous system causes neurodegeneration in mice. Nature 2006; 441:880-4; PMID:16625205; http://dx.doi.org/10.1038/nature04723
15. Komatsu M, Waguri S, Koike M, Sou YS, Ueno T, Hara T, Mizushima N, Iwata J, Ezaki J, Murata S, et al. Homeostatic levels of p62 control cytoplasmic inclusion body formation in autophagy-deficient mice. Cell 2007; 131:1149-63; PMID:18083104; http://dx.doi.org/10.1016/j.cell.2007.10.035
16. Komatsu M, Waguri S, Ueno T, Iwata J, Murata S, Tanida I, Ezaki J, Mizushima N, Ohsumi Y, Uchiyama Y, et al. Impairment of starvation-induced and constitutive autophagy in Atg7-deficient mice. J Cell Biol 2005; 169:425-34; PMID:15866887; http://dx.doi.org/10.1083/jcb.200412022
17. Murphy MP. How mitochondria produce reactive oxygen species. Biochem J 2009; 417:1-13; PMID:19061483; http://dx.doi.org/10.1042/BJ20081386
18. Kitada T, Asakawa S, Hattori N, Matsumine H, Yamamura Y, Minoshima S, Yokochi M, Mizuno Y, Shimizu N. Mutations in the parkin gene cause autosomal recessive juvenile parkinsonism. Nature 1998; 392:605-8; PMID:9560156; http://dx.doi.org/10.1038/33416
19. Narendra D, Tanaka A, Suen DF, Youle RJ. Parkin is recruited selectively to impaired mitochondria and promotes their autophagy. J Cell Biol 2008; 183:795-803; PMID:19029340; http://dx.doi.org/10.1083/jcb.200809125
20. Yoshii SR, Kishi C, Ishihara N, Mizushima N. Parkin mediates proteasome-dependent protein degradation and rupture of the outer mitochondrial membrane. J Biol Chem 2011; 286:19630-40; PMID:21454557; http://dx.doi.org/10.1074/jbc.M110.209338
21. Lokireddy S, Wijesoma IW, Teng S, Bonala S, Gluckman PD, McFarlane C, Sharma M, Kambadur R. The ubiquitin ligase Mul1 induces mitophagy in skeletal muscle in response to muscle-wasting stimuli. Cell Metab 2012; 16:613-24; PMID:23140641; http://dx.doi.org/10.1016/j.cmet.2012.10.005
22. Sato S, Chiba T, Nishiyama S, Kakiuchi T, Tsukada H, Hatano T, Fukuda T, Yasoshima Y, Kai N, Kobayashi K, et al. Decline of striatal dopamine release in parkin-deficient mice shown by ex vivo autoradiography. J Neurosci Res 2006; 84:1350-7; PMID:16941649; http://dx.doi.org/10.1002/jnr.21032
23. Cha GH, Kim S, Park J, Lee E, Kim M, Lee SB, Kim JM, Chung J, Cho KS. Parkin negatively regulates JNK pathway in the dopaminergic neurons of Drosophila. Proc Natl Acad Sci U S A 2005; 102:10345-50; PMID:16002472; http://dx.doi.org/10.1073/pnas.0500346102
24. Greene JC, Whitworth AJ, Kuo I, Andrews LA, Feany MB, Pallanck LJ. Mitochondrial pathology and apoptotic muscle degeneration in Drosophila parkin mutants. Proc Natl Acad Sci U S A 2003; 100:4078-83; PMID:12642658; http://dx.doi.org/10.1073/pnas.0737556100

25. Pesah Y, Pham T, Burgess H, Middlebrooks B, Verstreken P, Zhou Y, Harding M, Bellen H, Mardon G. Drosophila parkin mutants have decreased mass and cell size and increased sensitivity to oxygen radical stress. Development 2004; 131:2183-94; PMID:15073152; http://dx.doi.org/10.1242/dev.01095
26. Bence NF, Sampat RM, Kopito RR. Impairment of the ubiquitin-proteasome system by protein aggregation. Science 2001; 292:1552-5; PMID:11375494; http://dx.doi.org/10.1126/science.292.5521.1552
27. Korolchuk VI, Mansilla A, Menzies FM, Rubinsztein DC. Autophagy inhibition compromises degradation of ubiquitin-proteasome pathway substrates. Mol Cell 2009; 33:517-27; PMID:19250912; http://dx.doi.org/10.1016/j.molcel.2009.01.021
28. Bodine SC, Latres E, Baumhueter S, Lai VK, Nunez L, Clarke BA, Poueymirou WT, Panaro FJ, Na E, Dharmarajan K, et al. Identification of ubiquitin ligases required for skeletal muscle atrophy. Science 2001; 294:1704-8; PMID:11679633; http://dx.doi.org/10.1126/science.1065874
29. Gomes MD, Lecker SH, Jagoe RT, Navon A, Goldberg AL. Atrogin-1, a muscle-specific F-box protein highly expressed during muscle atrophy. Proc Natl Acad Sci U S A 2001; 98:14440-5; PMID:11717410; http://dx.doi.org/10.1073/pnas.251541198
30. Arlt A, Bauer I, Schafmayer C, Tepel J, Müerköster SS, Brosch M, Röder C, Kalthoff H, Hampe J, Moyer MP, et al. Increased proteasome subunit protein expression and proteasome activity in colon cancer relate to an enhanced activation of nuclear factor E2-related factor 2 (Nrf2). Oncogene 2009; 28:3983-96; PMID:19734940; http://dx.doi.org/10.1038/onc.2009.264
31. Kwak MK, Wakabayashi N, Greenlaw JL, Yamamoto M, Kensler TW. Antioxidants enhance mammalian proteasome expression through the Keap1-Nrf2 signaling pathway. Mol Cell Biol 2003; 23:8786-94; PMID:14612418; http://dx.doi.org/10.1128/MCB.23.23.8786-8794.2003
32. Radhakrishnan SK, Lee CS, Young P, Beskow A, Chan JY, Deshaies RJ. Transcription factor Nrf1 mediates the proteasome recovery pathway after proteasome inhibition in mammalian cells. Mol Cell 2010; 38:17-28; PMID:20385086; http://dx.doi.org/10.1016/j.molcel.2010.02.029
33. Steffen J, Seeger M, Koch A, Krüger E. Proteasomal degradation is transcriptionally controlled by TCF11 via an ERAD-dependent feedback loop. Mol Cell 2010; 40:147-58; PMID:20932482; http://dx.doi.org/10.1016/j.molcel.2010.09.012
34. Biswas M, Chan JY. Role of Nrf1 in antioxidant response element-mediated gene expression and beyond. Toxicol Appl Pharmacol 2010; 244:16-20; PMID:19665035; http://dx.doi.org/10.1016/j.taap.2009.07.034
35. Wang W, Chan JY. Nrf1 is targeted to the endoplasmic reticulum membrane by an N-terminal transmembrane domain. Inhibition of nuclear translocation and transacting function. J Biol Chem 2006; 281:19676-87; PMID:16687406; http://dx.doi.org/10.1074/jbc.M602802200
36. Zhang Y, Lucocq JM, Hayes JD. The Nrf1 CNC/bZIP protein is a nuclear envelope-bound transcription factor that is activated by t-butyl hydroquinone but not by endoplasmic reticulum stressors. Biochem J 2009; 418:293-310; PMID:18990090; http://dx.doi.org/10.1042/BJ20081575
37. Powers SK, Wiggs MP, Duarte JA, Zergeroglu AM, Demirel HA. Mitochondrial signaling contributes to disuse muscle atrophy. Am J Physiol Endocrinol Metab 2012; 303:E31-9; PMID:22395111; http://dx.doi.org/10.1152/ajpendo.00609.2011
38. Zhang Y, Lucocq JM, Yamamoto M, Hayes JD. The NHB1 (N-terminal homology box 1) sequence in transcription factor Nrf1 is required to anchor it to the endoplasmic reticulum and also to enable its asparagine-glycosylation. Biochem J 2007; 408:161-72; PMID:17705787; http://dx.doi.org/10.1042/BJ20070761
39. Cullinan SB, Gordan JD, Jin J, Harper JW, Diehl JA. The Keap1-BTB protein is an adaptor that bridges Nrf2 to a Cul3-based E3 ligase: oxidative stress sensing by a Cul3-Keap1 ligase. Mol Cell Biol 2004; 24:8477-86; PMID:15367669; http://dx.doi.org/10.1128/MCB.24.19.8477-8486.2004
40. Furukawa M, Xiong Y. BTB protein Keap1 targets antioxidant transcription factor Nrf2 for ubiquitination by the Cullin 3-Roc1 ligase. Mol Cell Biol 2005; 25:162-71; PMID:15601839; http://dx.doi.org/10.1128/MCB.25.1.162-171.2005
41. Kobayashi A, Kang MI, Okawa H, Ohtsuji M, Zenke Y, Chiba T, Igarashi K, Yamamoto M. Oxidative stress sensor Keap1 functions as an adaptor for Cul3-based E3 ligase to regulate proteasomal degradation of Nrf2. Mol Cell Biol 2004; 24:7130-9; PMID:15282312; http://dx.doi.org/10.1128/MCB.24.16.7130-7139.2004
42. Zhang DD, Lo SC, Cross JV, Templeton DJ, Hannink M. Keap1 is a redox-regulated substrate adaptor protein for a Cul3-dependent ubiquitin ligase complex. Mol Cell Biol 2004; 24:10941-53; PMID:15572695; http://dx.doi.org/10.1128/MCB.24.24.10941-10953.2004
43. Hayes JD, McMahon M. NRF2 and KEAP1 mutations: permanent activation of an adaptive response in cancer. Trends Biochem Sci 2009; 34:176-88; PMID:19321346; http://dx.doi.org/10.1016/j.tibs.2008.12.008
44. Motohashi H, Yamamoto M. Nrf2-Keap1 defines a physiologically important stress response mechanism. Trends Mol Med 2004; 10:549-57; PMID:15519281; http://dx.doi.org/10.1016/j.molmed.2004.09.003
45. Villeneuve NF, Lau A, Zhang DD. Regulation of the Nrf2-Keap1 antioxidant response by the ubiquitin proteasome system: an insight into cullin-ring ubiquitin ligases. Antioxid Redox Signal 2010; 13:1699-712; PMID:20486766; http://dx.doi.org/10.1089/ars.2010.3211
46. Tanahashi N, Murakami Y, Minami Y, Shimbara N, Hendil KB, Tanaka K. Hybrid proteasomes. Induction by interferon-gamma and contribution to ATP-dependent proteolysis. J Biol Chem 2000; 275:14336-45; PMID:10799514; http://dx.doi.org/10.1074/jbc.275.19.14336

Journal of Human Genetics (2013) 58, 259–266

www.nature.com/jhg

ORIGINAL ARTICLE

Exome sequencing identifies a novel *TTN* mutation in a family with hereditary myopathy with early respiratory failure

Rumiko Izumi[1,2], Tetsuya Niihori[1], Yoko Aoki[1], Naoki Suzuki[2], Masaaki Kato[2], Hitoshi Warita[2], Toshiaki Takahashi[3], Maki Tateyama[2], Takeshi Nagashima[4], Ryo Funayama[4], Koji Abe[5], Keiko Nakayama[4], Masashi Aoki[2] and Yoichi Matsubara[1]

Myofibrillar myopathy (MFM) is a group of chronic muscular disorders that show the focal dissolution of myofibrils and accumulation of degradation products. The major genetic basis of MFMs is unknown. In 1993, our group reported a Japanese family with dominantly inherited cytoplasmic body myopathy, which is now included in MFM, characterized by late-onset chronic progressive distal muscle weakness and early respiratory failure. In this study, we performed linkage analysis and exome sequencing on these patients and identified a novel c.90263G>T mutation in the *TTN* gene (NM_001256850). During the course of our study, another groups reported three mutations in *TTN* in patients with hereditary myopathy with early respiratory failure (HMERF, MIM #603689), which is characterized by overlapping pathologic findings with MFMs. Our patients were clinically compatible with HMERF. The mutation identified in this study and the three mutations in patients with HMERF were located on the A-band domain of titin, suggesting a strong relationship between mutations in the A-band domain of titin and HMERF. Mutation screening of *TTN* has been rarely carried out because of its huge size, consisting of 363 exons. It is possible that focused analysis of *TTN* may detect more mutations in patients with MFMs, especially in those with early respiratory failure.
Journal of Human Genetics (2013) **58**, 259–266; doi:10.1038/jhg.2013.9; published online 28 February 2013

Keywords: A-band; cytoplasmic body; Fn3 domain; hereditary myopathy with early respiratory failure; HMERF; myofibrillar myopathy; titin; *TTN*

INTRODUCTION

Myofibrillar myopathies (MFMs) were proposed in 1996 as a group of chronic muscular disorders characterized by common morphologic features observed on muscle histology, which showed the focal dissolution of myofibrils followed by the accumulation of products of the degradative process.[1] The clinical phenotype of MFM is characterized by slowly progressive muscle weakness that can involve proximal or distal muscles, with onset in adulthood in most cases. However, other phenotypes are highly variable. Although 20% of patients with MFMs have been revealed to have mutations in *DES*, *CRYAB*, *MYOT*, *LDB* (*ZASP*), *FLNC* or *BAG3*, the major genetic basis of MFMs remains to be elucidated.

Respiratory weakness is one of the symptoms of MFMs. The early or initial presentation of respiratory failure is not a common manifestation of MFMs as a whole, and there are limited reports regarding a fraction of patients with *DES*,[2] *MYOT*[3] or *CRYAB*[4] mutation. In 1993, our group reported a Japanese family with dominantly inherited cytoplasmic body (CB) myopathy,[5] which is now included in MFM. Currently, this family includes 20 patients in five successive generations who show almost homogeneous clinical features characterized by chronic progressive distal muscle weakness and early respiratory failure. However, the underlying genetic etiology in this family was unknown. The aim of this study was to determine the genetic cause in this family. To identify the responsible genetic mutation, we performed linkage analysis and whole-exome sequencing.

MATERIALS AND METHODS

This study was approved by the Ethics Committee of the Tohoku University School of Medicine, and all individuals gave their informed consent before their inclusion in the study.

[1]Department of Medical Genetics, Tohoku University School of Medicine, Sendai, Japan; [2]Department of Neurology, Tohoku University School of Medicine, Sendai, Japan; [3]Department of Neurology and Division of Clinical Research, National Hospital Organization Nishitaga National Hospital, Sendai, Japan; [4]Division of Cell Proliferation, United Centers for Advanced Research and Translational Medicine, Tohoku University Graduate School of Medicine, Sendai, Japan and [5]Department of Neurology, Okayama University Medical School, Okayama, Japan
Correspondence: Dr Y Aoki, Department of Medical Genetics, Tohoku University School of Medicine, 1-1 Seiryo-machi, Aoba-ku, Sendai 980-8574, Japan.
E-mail: aokiy@med.tohoku.ac.jp
or Professor M Aoki, Department of Neurology, Tohoku University School of Medicine, 1-1 Seiryo-machi, Aoba-ku, Sendai 980-8574, Japan.
E-mail: aokim@med.tohoku.ac.jp
Received 23 October 2012; revised 9 January 2013; accepted 10 January 2013; published online 28 February 2013

Clinical information on the family

This family includes 20 patients (13 males and 7 females) in five successive generations (Figure 1). The family is of Japanese ancestry, and no consanguineous or international mating was found. Of all patients, seven underwent a muscle biopsy, and two were autopsied. All of the histological findings were compatible with MFM (see clinical data).

The age of onset ranged from 27–45 years. The most common presenting symptom was foot drop. At the initial evaluations, muscle weakness was primarily distributed in the ankle dorsiflexors and finger extensors. The patients were generally built and showed no other extramuscular abnormalities. In addition to this chronic progressive distal muscle weakness, respiratory distress occurred between 0 and 7 years from the initial onset (average 3.8 years) in seven patients (IV-9, V-2, A, B, E, H, and J) with adequate clinical information. Two patients who had not had any respiratory care died of respiratory failure approximately a decade from the initial onset. The other patients have been alive for more than 10 years (maximum 18 years) but require nocturnal non-invasive positive pressure ventilation. They were 37–58 years of age as of 2012 and able to walk independently with or without a simple walking aid. Although the time at which patients recognized dysphagia or dysarthria varied between 1 to more than 10 years from the initial onset, decreased bulbar functions had been noted at the initial evaluation in most cases. Cardiac function was normally maintained in all patients of the family.

Clinical data

The level of serum creatine kinase was normal or mildly elevated. Electromyography of affected muscles showed a chronic myogenic pattern, and the nerve conduction study did not suggest any neuropathic involvement. Muscle imaging showed focal atrophy in the tibialis anterior, tibialis posterior, extensor hallucis and digitorum longus, peroneal and semitendinosus muscle on initial assessment (Figure 2A), and atrophy became clear in cervical muscles, shoulder girdles, intercostals and proximal limb muscles in the following several years. Upon muscle biopsy, the most common finding was numerous cytoplasmic bodies (CBs), which were found on 7.3% of myofibers in the tibialis anterior of individual E (Figure 2B (a–c)) and 50–80% of intercostals in other cases.[5] Other nonspecific findings were increased variability in the size of myofibers, central nuclei and rimmed vacuoles observed on a few fibers. No strong immunoreaction of desmin was seen in the CBs (Figure 2B (d, e)). An electron microscope examination showed that the regular sarcoplasmic pattern was replaced by abnormal fine filamentous structures, which seemed to attach to the Z-band. CBs were also found in almost all skeletal muscles and some smooth muscles in autopsied cases.[5] Cardiac myofibers also contained numerous CBs in one of the autopsied cases (V-2),[5] although the patient did not present any cardiac complication. The sequence analysis of the coding regions and flanking introns of *DES* and *MYOT* showed no pathogenic mutation in individual E. An array comparative genomic hybridization performed with the Agilent SurePrint G3 Human CGH 1M microarray format in individual A did not reveal any aberrations of genomic copy number.

Linkage analysis

DNA was extracted by standard methods. Linkage analysis was performed on nine family members (A–I in Figure 1; four of them were affected, and the others were unaffected) through genotyping using an Illumina Human Omni 2.5 BeadChip (Illumina, San Diego, CA, USA). We chose single-nucleotide polymorphisms (SNPs) that satisfied all of the following criteria: (1) autosomal SNPs whose allele frequencies were available from the HapMap project (http://hapmap.ncbi.nlm.nih.gov/), (2) SNPs that were not monomorphic among members and (3) SNPs that were not in strong linkage disequilibrium with neighboring SNPs (r2 values <0.9). Then, we selected the first five SNPs from each position of integer genetic distance from SNPs that met the above criteria for the initial analysis. The details were as follows; we chose a SNP closest to 0 cM and the neighboring four SNPs. If the genetic distance of a SNP was the same as that of the next SNP, we considered the genomic position to determine their order. We repeated this process at 1 cM, 2 cM and so on.

We performed a multipoint linkage analysis of the data set (17 613 SNPs) using MERLIN[6] 1.1.2 under the autosomal dominant mode with the following parameters: 0.0001 for disease allele frequency, 1.00 for individuals heterozygous and homozygous for the disease allele and 0.00 for individuals

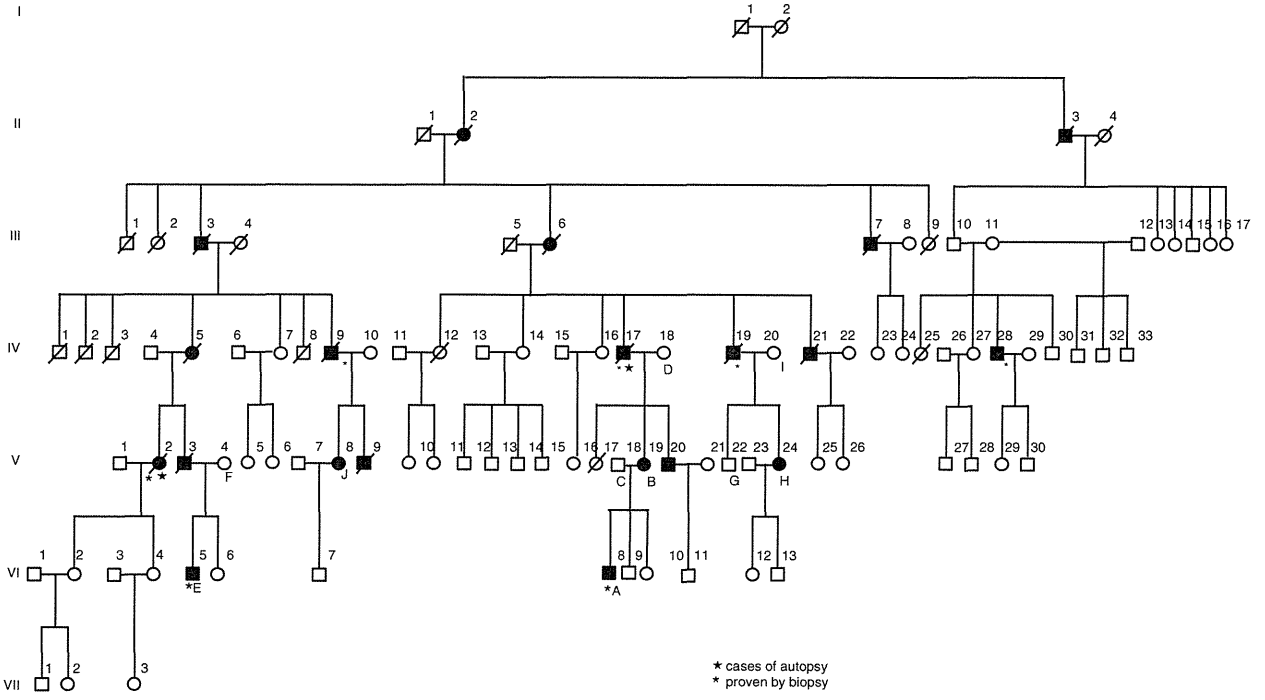

Figure 1 Family pedigree. Filled-in symbols indicate individuals with MFM. Empty symbols indicate unaffected individuals. A star and asterisk indicate autopsy-proven and muscle biopsy-proven cases, respectively. (A–J) indicates individuals whose DNA was used for this study.

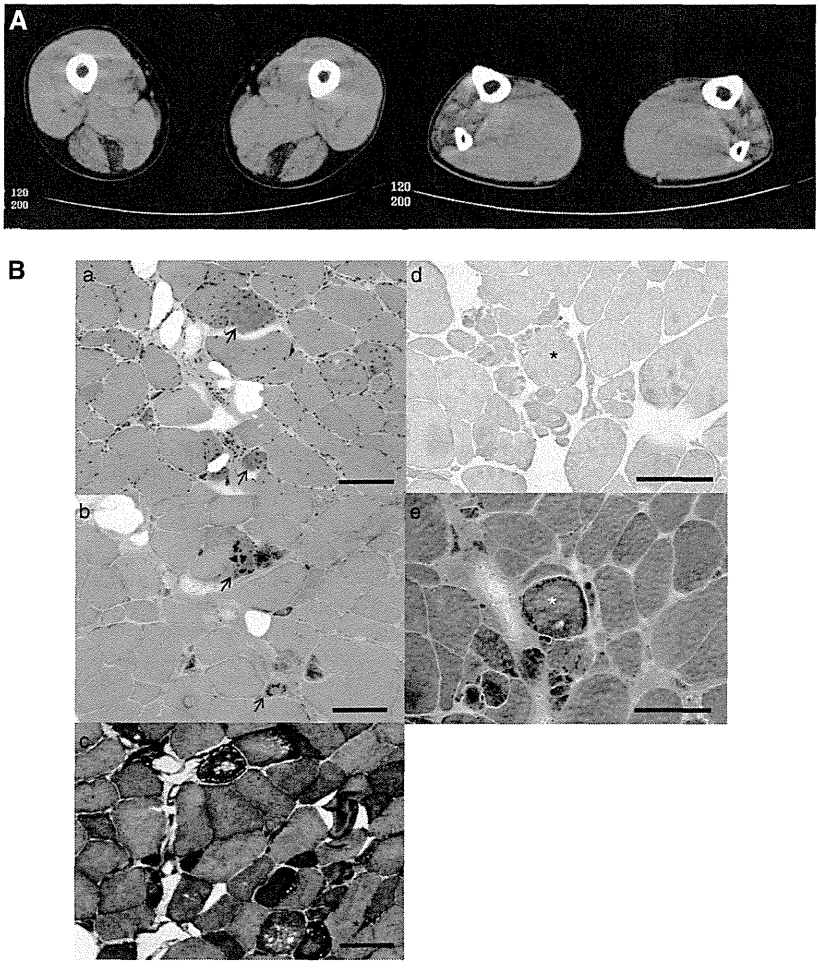

Figure 2 Family clinical data. (**A**) Muscle computed tomography of affected lower extremity. The imaging in the initial assessment of individual A showed symmetrical atrophy and fatty replacement of the semitendinosus in the proximal lower extremities (left) and the tibialis anterior, tibialis posterior, extensor hallucis and digitorum longus, and peroneal muscle in the distal (right) lower extremities. (**B**) Pathology of muscle biopsy. Hematoxylin-eosin (a), Gomori-trichrome (b) and NADH (nicotinamide adenine dinucleotide)-tetrazolium reductase (c) staining of the muscle biopsy sample from the tibialis anterior of individual E are shown. CBs are indicated by arrows. CBs were round or oval, 5–10 μm in diameter and predominantly located in the periphery of type 1 fibers, which stained eosinophilic with hematoxylin-eosin and blue–purple with Gomori-trichrome. NADH-tetrazolium reductase staining showed disorganization of the myofibrillar network. Immunostaining for desmin (d) and Gomori-trichrome staining (e) are serial sections of the muscle biopsy from individual E. Stars indicate corresponding fibers. No strong immunoreaction of desmin was seen in the CBs. Scale bars = 100 μm

homozygous for the alternative allele. After this first analysis, a second analysis was performed with all SNPs fulfilling the above criteria around the peaks identified in the first analysis.

Exome sequencing

Exome sequencing was performed on seven family members in three generations (A–E, H and I in Figure 1), four of whom were affected. Exon capture was performed with the SureSelect Human All Exon kit v2 (individuals E, H and I) or v4 (A–D) (Agilent Technologies, Santa Clara, CA, USA). Exon libraries were sequenced with the Illumina Hiseq 2000 platform according to the manufacturer's instructions (Illumina). Paired 101-base pair reads were aligned to the reference human genome (UCSChg19) using the Burrows-Wheeler Alignment tool.[7] Likely PCR duplicates were removed with the Picard program (http://picard.sourceforge.net/). Single-nucleotide variants and indels were identified using the Genome Analysis Tool Kit (GATK) v1.5 software.[8] SNVs and indels were annotated against the RefSeq database and dbSNP135 with the ANNOVAR program.[9] We used the PolyPhen2 polymorphism phenotyping software tool[10] to predict the functional effects of mutations.

Sanger sequencing

To confirm that mutations identified by exome sequencing segregated with the disease, we performed direct sequencing. PCR was performed with the primers shown in Supplementary Table 1. PCR products were purified with a MultiScreen PCR plate (Millipore, Billerica, MA, USA) and sequenced using BigDye terminator v1.1 and a 3500xL genetic analyzer (Applied Biosystems, Carlsbad, CA, USA).

RESULTS

Linkage analysis

The first linkage analysis identified five regions across autosomes with a logarithm of odds (LOD) score greater than 2 (Figure 3). Of the five regions, two were on chromosome 2 (from 167 cM to 168 cM, with a maximum LOD score of 2.46 and from 182 cM to 185 cM, with a maximum LOD score of 2.71), the other two were on chromosome 8 (from 27 cM to 34 cM, with a maximum LOD score of 2.71 and at 61 cM, with a maximum LOD score of 2.03), and one was on

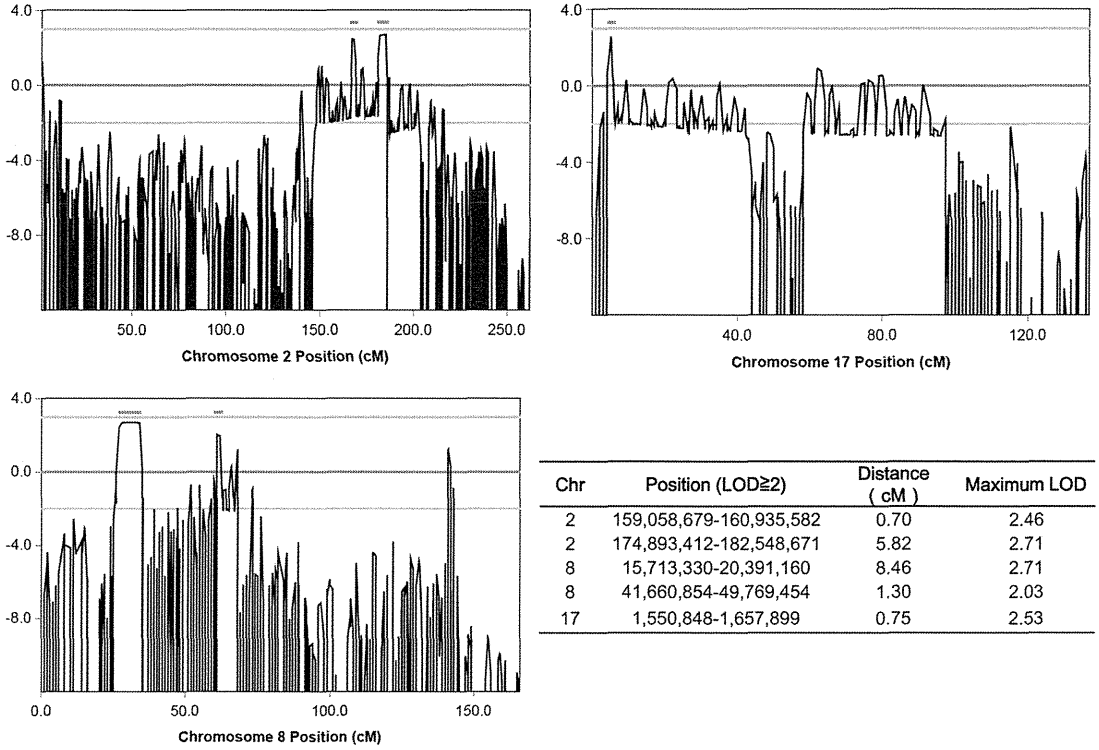

Chr	Position (LOD≧2)	Distance (cM)	Maximum LOD
2	159,058,679-160,935,582	0.70	2.46
2	174,893,412-182,548,671	5.82	2.71
8	15,713,330-20,391,160	8.46	2.71
8	41,660,854-49,769,454	1.30	2.03
17	1,550,848-1,657,899	0.75	2.53

Figure 3 Linkage analysis. Linkage analysis was performed on nine family members (four of them were affected, the others were unaffected) using an Illumina Human Omni 2.5 BeadChip. Five regions with an LOD score greater than 2 (indicated by bar) were identified. A full color version of this figure is available at the *Journal of Human Genetics* journal online.

Table 1 Summary of detected variants by exome sequencing

Individual *Morbidity*	*A* *Affected*	*B* *Affected*	*C* *Unaffected*	*D* *Unaffected*	*E* *Affected*	*H* *Affected*	*I* *Unaffected*	*Segregated in seven family members*
Exonic, splicing	10089	10064	10079	10065	10230	10194	10216	64
Nonsynonymous, splicing, indel, nonsense	4987	5020	5055	5038	5143	5234	5200	32
Allele frequency not available	577	600	536	555	671	794	786	2

chromosome 17 (at 5 cM, with a maximum LOD score of 2.53). In the second detailed linkage analysis, these peaks were determined to range from 167.49 cM at rs4233674 at position 159 058 679 to 168.19 cM at rs7598162 at position 160 935 582, and from 181.23 cM at rs4402725 at position 174 893 412 to 187.05 cM at rs7420169 at position 182 548 671 on chromosome 2; from 26.42 cM at rs2736043 at position 15 713 330 to 34.88 cM at rs9325871 at position 20 391 160, and from 61.02 cM at rs6999814 at position 41 660 854 to 62.32 cM at rs10957281 at position 49 769 454 on chromosome 8; and from 4.7 cM at rs11078552 at position 1 550 848 to 5.45 cM at rs1057355 at position 1 657 899 on chromosome 17. Haplotypes shared by affected individuals in these regions were confirmed by visual inspection. There were a few incompatible SNPs in these regions, presumably due to genotyping error.

Exome sequencing and segregation analysis

In exome sequencing, an average of 215 million reads enriched by SureSelect v4 (SSv4) and 319 million reads enriched by SureSelect v2 (SSv2) were generated, and 99% of reads were mapped to the reference genome by Burrows-Wheeler Alignment tool. An average of 57% (SSv4) and 61% (SSv2) of those reads were duplicated and removed, and an average of 80% (SSv4) and 66% (SSv2) of mapped reads without duplicates were in target regions. The average coverage of each exome was 163-fold (SSv4) and 130-fold (SSv2). An average of 85% (SSv4) and 69% (SSv2) of target regions were covered at least 50-fold (Supplementary Table 2). On average, 10 133 SNVs or indels, which are located within coding exons or splice sites, were identified per individual (Table 1). A total of 64 variants were common among patients and not present in unaffected individuals, and 32 of those were left after excluding synonymous SNVs. In these variants, only the heterozygous mutation c.90263G>T (NM_001256850) at position 179 410 777 of chromosome 2, which was predicted to p.W30088L in *TTN*, was novel (that is, not present in dbSNP v135 or 1000 genomes). Polyphen2 predicted this mutation as probably damaging. This mutation was located in a candidate region suggested by the linkage analysis in the present study. The other variants were registered with dbSNP135, and the allele frequencies, except for one SNV, rs138183879, in *IKBKB*, ranged from 0.0023 to 0.62.

a

Gene	Chr	Position	Variant type	Reference	Variant	dbSNP v135	Coding change	Prediction	Segregaion analysis
TTN	2	179 410777	Missense	G	T	Not present	W30088L	Probably damaging	Segregating
IKBKB	8	42 188 457	Missense	C	T	rs138183879	T742M	Benign	Non-segregating

b

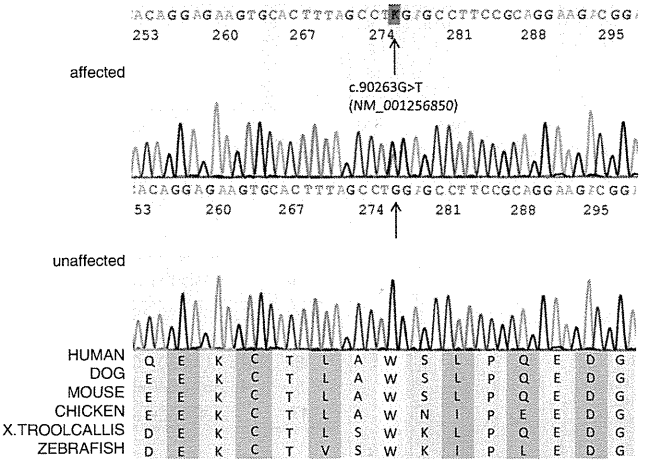

Figure 4 Identified mutations by exome sequencing. (**a**) We performed segregation analysis of two candidates. (**b**) The identified *TTN* mutation and its conservation among species. Sanger sequencing confirmed the heterozygous G to T substitution (indicated by the arrow) at the position chr2;179 410 777, which corresponds to c.90263G>T in exon 293 (NM_001256850.1). The substitution leads to p.W30088L (NP_001243779.1), and this amino acid is conserved among species.

These values were not compatible with the assumption that MFM was a rare disease and showed complete penetrance in this family. The allele frequency of rs138183879 was not available in dbSNP135, and this SNV was in the candidate region on chromosome 8 based on linkage analysis.

We then performed a segregation analysis on the two candidates, the novel mutation c.90263G>T in *TTN* and rs138183879 in *IKBKB*, through Sanger sequencing in 10 family members (A–J in Figure 1; Figure 4a). The rs138183879 SNP was not found in individual J, that is, it was not segregated with the disease in this family. In contrast, the novel mutation c.90263G>T in *TTN* was detected in all patients ($n=5$) and not detected in any of the unaffected family members ($n=5$) or 191 ethnically matched control subjects (382 chromosomes). These results suggested that this rare mutation in *TTN* segregated with the disease in this family.

DISCUSSION

In this study, we found that a novel missense mutation in *TTN* segregated with MFM in a large Japanese family. The identified c.90263G>T mutation in *TTN* (NM_001256850) was considered to be the genetic cause of MFM in our family, because (1) exome sequencing revealed that this was the best candidate mutation after filtering SNPs and indels, (2) this mutation is located in a region on chromosome 2 shared by affected family members, (3) the segregation with MFM was confirmed by Sanger sequencing, (4) this mutation was not detected in 191 control individuals, (5) this mutation was predicted to alter highly conserved amino acids (Figure 4b) and (6) *TTN* encodes a Z-disc-binding molecule called titin, which is similar to all of the previously identified causative genes for MFMs, which also encode Z-disc-associated molecules.

Recently, three mutations in *TTN* have been reported as the causes of hereditary myopathy with early respiratory failure (HMERF, MIM #603689),[11–16] which has similar muscle pathology to MFMs. The identified novel missense mutation c.90263G>T in our study was located on the same exon as recently reported HMERF mutations: c.90272C>T in a Portuguese family[16] and c.90315T>C in Swedish and English families[14,15] (Table 2). This finding suggests the possibility that our family can be recognized as having HMERF from a clinical aspect.

Compared with symptoms described in the past three reports on HMERF (also see Table 2), our patients have common features, such as autosomal dominant inheritance, early respiratory failure, the absence of clinically apparent cardiomyopathy, normal to mild elevation of serum CK and histological findings compatible with MFM. Early involvement of the tibialis anterior is also common, except for the Portuguese family, who reported isolated respiratory insufficiency and a milder presentation of HMERF. Thus, our family shares major clinical manifestations with patients with HMERF, suggesting that the identified mutation is novel for MFM and HMERF.

To date, mutations in *TTN* have been identified in skeletal myopathy and cardiomyopathy.[17,18] The relationship between the variant positions on *TTN* and phenotypes accompanied by skeletal or respiratory muscle involvement is summarized in Table 2. Titin is a large protein (4.20 MDa) that extends from the Z-disk to the M-line within the sarcomere, and it is composed of four major domains: Z-disc, I-band, A-band and M-line (Figure 5). All four HMERF mutations detected by other groups and our study were consistently located in the A-band domain, while mutations in tibial muscular dystrophy (TMD) (MIM #600334),[19–24] limb-girdle muscular dystrophy type 2J (LGMD2J) (#608807)[19,25] and early-onset myopathy with fatal cardiomyopathy (#611705)[26] were located in the M-line domain. HMERF and TMD have some common clinical characteristics, such as autosomal dominant inheritance with onset in adulthood and strong involvement of the tibialis anterior muscle.

Table 2 Previously reported TTN mutations with skeletal and/or respiratory muscle involvement

Phenotype	*LGMD*	*HMERF*	*Our family*	*HMERF*	*HMERF*	*TMD*	*TMD*	*LGMD2J*	*TMD*	*TMD*	*TMD*	*TMD*	*TMD*	*Early-onset myopathy with fatal cardiomyopathy*	*Early-onset myopathy with fatal cardiomyopathy*
Reported by	Vasli *et al.*[16]	Ohlsson *et al.*,[14] Pfeffer *et al.*[15]	Abe *et al.*[5]	Vasli *et al.*[16]	Edstrom *et al.*,[12] Nicolao, *et al.*[11] Lang e *et al.*[13]	Hackman *et al.*[23]	Udd *et al.*,[20] Hackman *et al.*[19]	Udd *et al.*,[25] Hackman *et al.*[19]	Pollazzon *et al.*[24]	Van den Bergh *et al.*[22]	Seze *et al.*,[21] Hackman *et al.*[19]	Hackman *et al.*[23]	Hackman *et al.*[23]	Carmignac *et al.*[26]	Carmignac *et al.*[26]
Mutation identified in Nucleotide (NM_001256850.1)	2012 c.3100G>A, c.52024G>A	2012 c.90315T>C	2012 c.90263G>T	2012 c.90272C>T	2005 c.97348C>T	2008 c.102724delT	2002 102857_ 102867 del11ins11	2002 102857_ 102867 del11ins11	2010 c.102914A>C	2003 c.102917T>A	2002 c.102944T>C	2008 c.102966delA	2008 c.102967C>T	2007 g.289385del ACCAAGTG	2007 g.291297delA
Protein (NP_001243779.1)	p.V1034M, p.A17342T	p.C30071R	p.W30088L	p.P30091L	p.R32450W				p.H34305P	p.I34306N	p.L34315P		p.Q34323X		
Domain	I-band, A-band	A-band (Fn3)	A-band (Fn3)	A-band (Fn3)	A-band (kinase)	M-line	M-line	M-line	M-line	M-line	M-line	M-line	M-line	M-line	M-line
Population	French	Swedish English	Japanese	Portuguese	Swedish	French	Finnish	Finnish	Italian	Belgian	French	Spanish	French	Sudanese	Moroccan
Inheritance	AR	AD	AD	AD	AD	AD	AD	AR	AD	AD	AD	AD	AD	Consanguineous siblings	Consanguineous siblings
Onset	35	33–71	27–45	46	20–50s	20–30s	35–55	20–30s	50–60s	47	45	40–50s	30s	Neonatal	Infant-early childhood
Skeletal muscles															
Major	Proximal UL and LL	TA, PL, EDL, ST	TA, ST	No	TA, neck flexor, proximals	TA, GA,HAM, pelvic	TA	All proximals	TA	TA	TA	TA	TA, HAM, pelvic	General muscle weakness and hypotonia	Psoas, TA, GA, peroneus
Minor		Neck flexor	Cervical, shoulder girdles, intercostals, proximal limb			QF				EDL, peroneal, TP	GA, femoral, scapular	HAM, GA	GA, distal UL		QF, proximal UL, neck, facial, trunk flexor
Spared			Facial			Proximal UL	Facial, UL, proximals	Facial		UL, proximal LL	Facial	UL	Proximal UL, QF		
Cardiac muscles	ND	No	No	ND	ND	ND	No	No	ND	ND	ND	ND	ND	DCM, onset; in the first decade	DCM, onset; 5–12 years old
Respiratory failure	ND	Yes, within 5–8 years	Yes, within 7 years	Isolated respiratory failure	Yes, as first presentation	ND	ND	ND	ND	ND	ND	ND	ND	ND	ND
Muscle pathologic features	ND	Inclusion bodies (major) and RVs (minor)	Cytoplasmic bodies (major) and RVs (minor)	Cytoplasmic bodies	Cytoplasmic bodies, positive for rhodamine-conjugated phalloidin	Dystrophic pattern without vacuoles	Nonspecific dystrophic change	Nonspecific dystrophic change, loss of calpain-3	Dystrophic pattern with RVs	Nonspecific, RV	Nonspecific	Dystrophic pattern with RVs	Nonspecific	Minicore-like lesions and abundant central nuclei	Minicore-like lesions and abundant central nuclei

Abbreviations: AD, autosomal dominant; AR, autosomal recessive; DCM, dilated cardiomyopathy; EDL, extensor digitorum longus; GA, gastrocnemius; HAM, hamstrings; LL, lower limb; ND, not described; no, no involvement; PL, peroneus longus; QF, quadriceps femoris; RV, rimmed vacuole;
ST, semitendinosus; TA, tibialis anterior; TMD, tibial muscular dystrophy; TP, tibialis posterior; UL, upper limb.

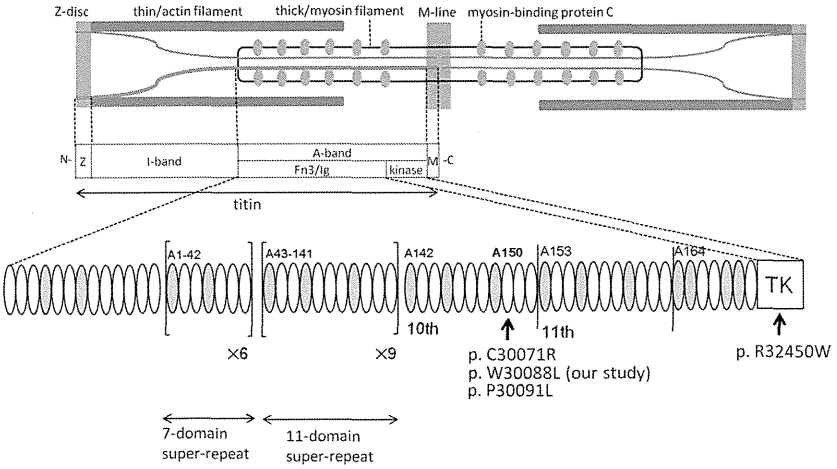

Figure 5 Structure of titin and mutation distribution in the A-band domain. Human *TTN* was mapped to 2q31.2. *TTN* is 294 kb and is composed of 363 exons that code for a maximum of 38 138 amino-acid residues and a 4.20-MDa protein[32] called titin. Titin is expressed in the cardiac and skeletal muscles and spans half the sarcomere, with its N-terminal at the Z-disc and the C-terminal at the M-line.[33] Titin is composed of four major domains: Z-disc, I-band, A-band and M-line. I-band regions of titin are thought to make elastic connections between the thick filament (that is, myosin filament) and the Z-disc within the sarcomere, whereas the A-band domain of titin seems to be bound to the thick filament, where it may regulate filament length and assembly.[34] The gray and white ellipses indicate an Ig-like domain and fibronectin type 3 domain, respectively. Our mutation (p.W30088L) and the neighboring two mutations (that is, p.C30071R and p.P30091L) were all located in the 6th Fn3 domain in the 10th domain of large super-repeats. A full color version of this figure is available at the *Journal of Human Genetics* journal online.

In contrast, one of the distinctive features of TMD is that early respiratory failure has not been observed in patients with TMD. Histological findings of TMD usually do not include CBs but show nonspecific dystrophic change. The underlying pathogenic processes explaining why mutations on these neighboring domains share some similarities but also some differences are unknown.

Three of four HMERF mutations in the A-band domain are located in the fibronectin type 3 and Ig-like (Fn3/Ig) domain, and one of four HMERF mutations is located in the kinase domain (Table 2, also see Figure 5). The missense mutation c.97348C>T in the kinase domain was the first reported HMERF mutation. It has been shown that the kinase domain has an important role in controlling muscle gene expression and protein turnover via the neighbor of BRCA1 gene-1-muscle-specific RING finger protein-serum response transcription factor pathway.[13] Moreover, the Fn3/Ig domain is composed of two types of super-repeats: six consecutive copies of 7-domain super-repeat at the N-terminus and 11 consecutive copies of 11-domain super-repeat at the C-terminus.[27–29] These super-repeats are highly conserved among species and muscles. Our identified mutation (c.90263G>T) and the neighboring two mutations (that is, c.90272C>T and c.90315T>C shown in Table 2) were all located on the 6th Fn3 domain in the 10th copy of 11-domain super-repeat (that is, A150 domain[30]) (Figure 5). Although some Fn3 domains are proposed to be the putative binding site for myosin,[31] the role with the majority of Fn3 domains, how it supports the structure of each repeat architecture, and the identity of its binding partner have not been fully elucidated. Our findings suggested that the Fn3 domain, in which mutations clustered, has critical roles in the pathogenesis of HMERF, although detailed mechanisms of pathogenesis remain unknown.

In conclusion, we have identified a novel disease-causing mutation in *TTN* in a family with MFM that was clinically compatible with HMERF. Because of its large size, global mutation screening of *TTN* has been difficult. Mutations in *TTN* may be detected by massively parallel sequencing in more patients with MFMs, especially in patients with early respiratory failure. Further studies are needed to understand the genotype–phenotype correlations in patients with mutations in *TTN* and the molecular function of titin.

ACKNOWLEDGEMENTS

We thank the patients and their family. We are grateful to Yoko Tateda, Kumi Kato, Naoko Shimakura, Risa Ando, Riyo Takahashi, Miyuki Tsuda, Nozomi Koshita, Mami Kikuchi and Kiyotaka Kuroda for their technical assistance. We also acknowledge the support of the Biomedical Research Core of Tohoku University Graduate School of Medicine. This work was supported by a grant of Research on Applying Health Technology provided by the Ministry of Health, Labor and Welfare to YM, an Intramural Research Grant (23-5) for Neurological and Psychiatric Disorders of NCNP and JSPS KAKENHI Grant number 24659421.

1 Nakano, S., Engel, A. G., Waclawik, A. J., Emslie-Smith, A. M. & Busis, N. A. Myofibrillar myopathy with abnormal foci of desmin positivity. I. Light and electron microscopy analysis of 10 cases. *J. Neuropathol. Exp. Neurol.* **55,** 549–562 (1996).
2 Olive, M., Odgerel, Z., Martinez, A., Poza, J. J., Bragado, F. G., Zabalza, R. J. *et al.* Clinical and myopathological evaluation of early- and late-onset subtypes of myofibrillar myopathy. *Neuromuscul. Disord.* **21,** 533–542 (2011).
3 Olive, M., Goldfarb, L. G., Shatunov, A., Fischer, D. & Ferrer, I. Myotilinopathy: refining the clinical and myopathological phenotype. *Brain* **128,** 2315–2326 (2005).
4 Selcen, D. & Engel, A. G. Myofibrillar myopathy caused by novel dominant negative alpha B-crystallin mutations. *Ann. Neurol.* **54,** 804–810 (2003).
5 Abe, K., Kobayashi, K., Chida, K., Kimura, N. & Kogure, K. Dominantly inherited cytoplasmic body myopathy in a Japanese kindred. *Tohoku. J. Exp. Med.* **170,** 261–272 (1993).
6 Abecasis, G. R., Cherny, S. S., Cookson, W. O. & Cardon, L. R. Merlin–rapid analysis of dense genetic maps using sparse gene flow trees. *Nat. Genet.* **30,** 97–101 (2002).
7 Li, H. & Durbin, R. Fast and accurate short read alignment with Burrows-Wheeler transform. *Bioinformatics* **25,** 1754–1760 (2009).
8 McKenna, A., Hanna, M., Banks, E., Sivachenko, A., Cibulskis, K., Kernytsky, A. *et al.* The Genome Analysis Toolkit: a MapReduce framework for analyzing next-generation DNA sequencing data. *Genome. Res.* **20,** 1297–1303 (2010).
9 Wang, K., Li, M. & Hakonarson, H. ANNOVAR: functional annotation of genetic variants from high-throughput sequencing data.. *Nucleic Acids Res.* **38,** e164 (2010).
10 Adzhubei, I. A., Schmidt, S., Peshkin, L., Ramensky, V. E., Gerasimova, A., Bork, P. *et al.* A method and server for predicting damaging missense mutations. *Nat. Methods* **7,** 248–249 (2010).
11 Nicolao, P., Xiang, F., Gunnarsson, L. G., Giometto, B., Edstrom, L., Anvret, M. *et al.* Autosomal dominant myopathy with proximal weakness and early respiratory muscle involvement maps to chromosome 2q. *Am. J. Hum. Genet.* **64,** 788–792 (1999).

12 Edstrom, L., Thornell, L. E., Albo, J., Landin, S. & Samuelsson, M. Myopathy with respiratory failure and typical myofibrillar lesions. *J. Neurol. Sci.* **96,** 211–228 (1990).
13 Lange, S., Xiang, F., Yakovenko, A., Vihola, A., Hackman, P., Rostkova, E. *et al.* The kinase domain of titin controls muscle gene expression and protein turnover. *Science* **308,** 1599–1603 (2005).
14 Ohlsson, M., Hedberg, C., Bradvik, B., Lindberg, C., Tajsharghi, H., Danielsson, O. *et al.* Hereditary myopathy with early respiratory failure associated with a mutation in A-band titin. *Brain* **135,** 1682–1694 (2012).
15 Pfeffer, G., Elliott, H. R., Griffin, H., Barresi, R., Miller, J., Marsh, J. *et al.* Titin mutation segregates with hereditary myopathy with early respiratory failure. *Brain* **135,** 1695–1713 (2012).
16 Vasli, N., Bohm, J., Le Gras, S., Muller, J., Pizot, C., Jost, B. *et al.* Next generation sequencing for molecular diagnosis of neuromuscular diseases. *Acta. Neuropathol.* **124,** 273–283 (2012).
17 Kontrogianni-Konstantopoulos, A., Ackermann, M. A., Bowman, A. L., Yap, S. V. & Bloch, R. J. Muscle giants: molecular scaffolds in sarcomerogenesis. *Physiol. Rev.* **89,** 1217–1267 (2009).
18 Ottenheijm, C. A. & Granzier, H. Role of titin in skeletal muscle function and disease. *Adv. Exp. Med. Biol.* **682,** 105–122 (2010).
19 Hackman, P., Vihola, A., Haravuori, H., Marchand, S., Sarparanta, J., De Seze, J. *et al.* Tibial muscular dystrophy is a titinopathy caused by mutations in TTN, the gene encoding the giant skeletal-muscle protein titin. *Am. J. Hum. Genet.* **71,** 492–500 (2002).
20 Udd, B., Partanen, J., Halonen, P., Falck, B., Hakamies, L., Heikkila, H. *et al.* Tibial muscular dystrophy. Late adult-onset distal myopathy in 66 Finnish patients. *Arch. Neurol.* **50,** 604–608 (1993).
21 de Seze, J., Udd, B., Haravuori, H., Sablonniere, B., Maurage, C. A., Hurtevent, J. F. *et al.* The first European family with tibial muscular dystrophy outside the Finnish population. *Neurology* **51,** 1746–1748 (1998).
22 Van den Bergh, P. Y., Bouquiaux, O., Verellen, C., Marchand, S., Richard, I., Hackman, P. *et al.* Tibial muscular dystrophy in a Belgian family. *Ann. Neurol.* **54,** 248–251 (2003).
23 Hackman, P., Marchand, S., Sarparanta, J., Vihola, A., Penisson-Besnier, I., Eymard, B. *et al.* Truncating mutations in C-terminal titin may cause more severe tibial muscular dystrophy (TMD). *Neuromuscul. Disord.* **18,** 922–928 (2008).
24 Pollazzon, M., Suominen, T., Penttila, S., Malandrini, A., Carluccio, M. A., Mondelli, M. *et al.* The first Italian family with tibial muscular dystrophy caused by a novel titin mutation. *J. Neurol.* **257,** 575–579 (2010).
25 Udd, B., Rapola, J., Nokelainen, P., Arikawa, E. & Somer, H. Nonvacuolar myopathy in a large family with both late adult onset distal myopathy and severe proximal muscular dystrophy. *J. Neurol. Sci.* **113,** 214–221 (1992).
26 Carmignac, V., Salih, M. A., Quijano-Roy, S., Marchand, S., Al Rayess, M. M., Mukhtar, M. M. *et al.* C-terminal titin deletions cause a novel early-onset myopathy with fatal cardiomyopathy. *Ann. Neurol.* **61,** 340–351 (2007).
27 Labeit, S., Barlow, D. P., Gautel, M., Gibson, T., Holt, J., Hsieh, C. L. *et al.* A regular pattern of two types of 100-residue motif in the sequence of titin. *Nature* **345,** 273–276 (1990).
28 Labeit, S. & Kolmerer, B. Titins: giant proteins in charge of muscle ultrastructure and elasticity. *Science* **270,** 293–296 (1995).
29 Tskhovrebova, L., Walker, M. L., Grossmann, J. G., Khan, G. N., Baron, A. & Trinick, J. Shape and flexibility in the titin 11-domain super-repeat. *J. Mol. Biol.* **397,** 1092–1105 (2010).
30 Bucher, R. M., Svergun, D. I., Muhle-Goll, C. & Mayans, O. The structure of the FnIII Tandem A77-A78 points to a periodically conserved architecture in the myosin-binding region of titin. *J. Mol. Biol.* **401,** 843–853 (2010).
31 Muhle-Goll, C., Habeck, M., Cazorla, O., Nilges, M., Labeit, S. & Granzier, H. Structural and functional studies of titin's fn3 modules reveal conserved surface patterns and binding to myosin S1–a possible role in the Frank-Starling mechanism of the heart. *J. Mol. Biol.* **313,** 431–447 (2001).
32 Bang, M. L., Centner, T., Fornoff, F., Geach, A. J., Gotthardt, M., McNabb, M. *et al.* The complete gene sequence of titin, expression of an unusual approximately 700-kDa titin isoform, and its interaction with obscurin identify a novel Z-line to I-band linking system. *Circ. Res.* **89,** 1065–1072 (2001).
33 Maruyama, K., Yoshioka, T., Higuchi, H., Ohashi, K., Kimura, S. & Natori, R. Connectin filaments link thick filaments and Z lines in frog skeletal muscle as revealed by immunoelectron microscopy. *J. Cell. Biol.* **101,** 2167–2172 (1985).
34 Guo, W., Bharmal, S. J., Esbona, K. & Greaser, M. L. Titin diversity–alternative splicing gone wild. *J. Biomed. Biotechnol.* **2010,** 753675 (2010).

Supplementary Information accompanies the paper on Journal of Human Genetics website (http://www.nature.com/jhg)

Clinical Neurology and Neurosurgery 115 (2013) 1555–1557

Contents lists available at SciVerse ScienceDirect

Clinical Neurology and Neurosurgery

journal homepage: www.elsevier.com/locate/clineuro

Case report

Autopsy-confirmed progressive supranuclear palsy with decreased uptake of metaiodobenzylguanidine

Tadashi Adachi[a,*], Michio Kitayama[a], Kenji Wada-Isoe[a], Toshiya Nakano[a], Kenji Nakashima[a]

[a] Division of Neurology, Department of Brain and Neurosciences, Faculty of Medicine, Tottori University, Yonago, Japan

ARTICLE INFO

Article history:
Received 4 September 2011
Received in revised form 5 January 2013
Accepted 12 January 2013
Available online 5 February 2013

Keywords:
Progressive supranuclear palsy
MIBG
Pathology

1. Introduction

Progressive supranuclear palsy (PSP) is a clinical syndrome comprising supranuclear gaze palsy, postural instability, and dementia. In clinical practice, it is sometimes difficult to distinguish between PSP, early-stage Parkinson's disease (PD), or multiple system atrophy. In the context of these difficulties, decreased cardiac uptake of metaiodobenzylguanidine (MIBG), a physiological analog of norepinephrine, has been reported in patients with PD and dementia with Lewy bodies [1,2]. Some patients with PSP also show slightly reduced MIBG uptake in comparison to healthy controls [3]; however, pathological analyses of these cases have not been conducted. Here, we investigated a case of autopsy-confirmed PSP with decreased MIBG uptake.

2. Case report

This male patient was age 76 at time of death. He was healthy while employed at an office and there was no family history of neurological disorders. At age 69, he had difficulty in walking and looking downward when he was putting on shoes. At the same time, his family noticed him becoming forgetful. He was initially diagnosed with PD and he received L-DOPA/decarboxylase inhibitor (300 mg/day) without effect. Gradually, his gait became unstable and he fell often. At age 72, he was admitted to our hospital. He showed supranuclear vertical gaze palsy, rigidity of neck and extremities without asymmetry, akinesia, postural instability, and dementia (Mini-mental state examination score: 19/30). He showed no apraxia, agnosia, aphasia, or cerebellar signs. He showed no orthostatic hypotension, but suffered from neurogenic bladder. Brain MRI showed atrophy of the midbrain tegmentum (Fig. 1A). Single-photon emission tomography showed hypoperfusion in the frontal lobe. He was diagnosed with possible PSP according to the National Institute of Neurological Disorders and the Society for PSP criteria [4]. Two years after this diagnosis, the patient could not walk and speak. Hemoglobin A1c level, brain natriuretic peptide level, and cardiothoracic ratio on chest radiography were all within normal limits. Cerebrospinal fluid, electrocardiography, coefficient of variation of the R–R interval, and echocardiography all showed no abnormalities. To confirm whether he had concomitant PD pathology or not, we performed MIBG scintigraphy. MIBG scintigraphy performed one month before his death showed decreased cardiac uptake; the heart-to-mediastinum ratio was 1.71 (mean ratio of control patients in our institute ± SD: 2.23 ± 0.31 [5]) in the early image and 1.32 (2.16 ± 0.41) in the delayed image; washout rate was 45.9% (32.4 ± 7.9) (Fig. 1B and C). Drugs that may affect MIBG uptake, such as tricyclic and tetracyclic antidepressants, serotonin reuptake inhibitors, sympathomimetics, sympatholytics, and calcium channel antagonists, were not administered. Monoamine oxidase inhibitor was administered for one year until the patient was age 75. He died of pneumonia at age 76.

An autopsy was performed 12 h after death. The general autopsy revealed severe pneumonia. There was no myocardial infarction. The brain weighed 1200 g after fixation. Gross examination confirmed mild frontal atrophy. The midbrain tegmentum showed

* Corresponding author at: Division of Neurology, Department of Brain and Neurosciences, Faculty of Medicine, Tottori University, 36-1 Nishi-chou, Yonago 683-8504, Japan. Tel.: +81 859 38 6757; fax: +81 859 38 6759.
E-mail address: adachi.neuro@gmail.com (T. Adachi).

0303-8467/$ – see front matter
http://dx.doi.org/10.1016/j.clineuro.2013.01.004

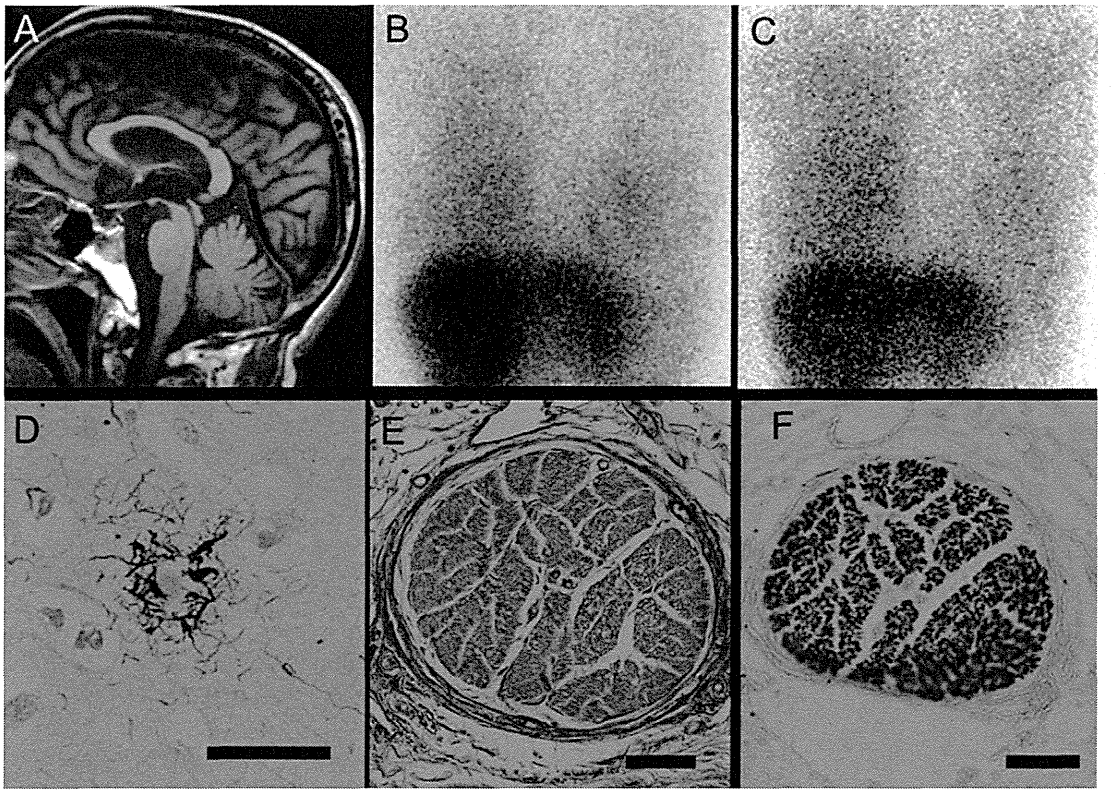

Fig. 1. Clinical images and pathologic findings. (A) Sagittal T2-weighted brain MRI shows severe atrophy of the midbrain tegmentum. The heart-to-mediastinum ratio for the post-injection metaiodobenzylguanidine scan was 1.71 in the early image (B) and 1.32 in the delayed image (C); washout rate was 45.9%. (D) Gallyas–Braak-positive, tuft-shaped astrocytes were present in the putamen; scale bar = 30 μm. Nerve bundles in the left ventricular wall were well preserved as shown by Azan staining (E) and by immunohistochemistry for phosphorylated neurofilament (F); scale bars = 60 μm.

marked atrophy, and the substantia nigra and locus coeruleus showed pigmentation loss. The subthalamic and red nuclei showed atrophy and grayish discoloration. Representative areas of formalin-fixed, paraffin-embedded brain tissue were sectioned and stained with hematoxylin and eosin (HE) and Klüver–Barrera staining. Selected sections were subjected to Gallyas–Braak silver staining. Cardiac left ventricle tissues were sectioned and stained with HE and Azan staining. For immunohistochemistry, we used antibodies to phosphorylated tau (AT8; Innogenetics, Temse, Belgium; 1:1000), β-amyloid 11–28 (12B2; IBL, Maebashi, Japan; 1:1000), phosphorylated α-synuclein (#64; Wako, Osaka, Japan; 1:5000), tyrosine hydroxylase (TH16; Sigma–Aldrich, MO, USA; 1:3000), and phosphorylated neurofilament (SMI-31; Sternberger, Baltimore, USA; 1:10,000). Peroxidase labeling was visualized with diaminobenzidine.

Microscopy showed neuronal loss and gliosis were severe in the globus pallidus, subthalamic nucleus, substantia nigra, dentate nucleus, and inferior olivary nucleus. Tuft-shaped astrocytes were scattered in the putamen, globus pallidus, red nucleus, and superior colliculus (Fig. 1D). Globoid type neurofibrillary tangles (NFT) were prominent in the midbrain, pons, medulla, and dentate nucleus. The neuropathologic diagnosis was definite PSP. Alzheimer-type pathology was minimal (Braak amyloid stage A and NFT stage I). There was no Lewy body–related α-synucleinopathy in the amygdala, dorsal nucleus of vagus, locus coeruleus, substantia nigra, transentorhinal cortex, hippocampus, or anterior cingulate gyrus. Sympathetic ganglia were not collected at autopsy. Nerve bundles of the epicardium and myocardium were well preserved as shown by azan staining and immunostaining for phosphorylated neurofilament and tyrosine hydroxylase (Fig. 1E and F).

3. Discussion

We present a case of autopsy-confirmed PSP with a clinically identified decrease in cardiac MIBG uptake. In Lewy body disease, cardiac sympathetic denervation precedes neuronal loss in the sympathetic ganglia [2] and decreased MIBG uptake has been established as a biomarker of Lewy body pathology *in vivo*. Decreased MIBG uptake has also been reported in some cases of PSP; concomitant PD pathology, involvement of the autonomic nervous system, and cardiovascular events have been postulated as causes [3]. These causes are unrelated to the present case and pathologically the cardiac nerves were well preserved. Functional abnormalities of the cardiac sympathetic nerve terminal may be responsible for the decreased MIBG uptake. For example, in the early scintigraphy image, dysfunction of noradrenergic transporters or monoamine transporters, or antagonism between MIBG and norepinephrine could be responsible for decreased MIBG uptake. In the delayed image, increased exocytosis due to hyperactivity of sympathetic function, reduced reuptake due to dysfunction of monoamine transporters could be responsible for decreased MIBG uptake. Proving the presence of these conditions with the neuropathological methods currently available is difficult; however, it is possible to evaluate cardiac nerve denervation. These conditions may be present in PSP or in only the akinetic mutism state like in the present case. We should examine many more cases of autopsy-proven PSP cases that include MIBG scintigraphy in clinical practice.

4. Conclusion

This case provides important information about the interpretation of MIBG scintigraphy in clinical practice.

References

[1] Orimo S, Ozawa E, Nakade S, Sugimoto T, Mizusawa H. (123)I-metaiodobenzylguanidine myocardial scintigraphy in Parkinson's disease. Journal of Neurology, Neurosurgery and Psychiatry 1999;67:189–94.
[2] Orimo S, Amino T, Itoh Y, Takahashi A, Kojo T, Uchihara T, et al. Cardiac sympathetic denervation precedes neuronal loss in the sympathetic ganglia in Lewy body disease. Acta Neuropathologica 2005;109:583–8.
[3] Yoshita M. Differentiation of idiopathic Parkinson's disease from striatonigral degeneration and progressive supranuclear palsy using iodine-123 meta-iodobenzylguanidine myocardial scintigraphy. Journal of the Neurological Sciences 1998;155:60–7.
[4] Litvan I, Agid Y, Calne D, Campbell G, Dubois B, Duvoisin RC, et al. Clinical research criteria for the diagnosis of progressive supranuclear palsy (Steele–Richardson–Olszewski syndrome): report of the NINDS-SPSP international workshop. Neurology 1996;47:1–9.
[5] Wada-Isoe K, Kitayama M, Nakaso K, Nakashima K. Diagnostic markers for diagnosing dementia with Lewy bodies: CSF and MIBG cardiac scintigraphy study. Journal of the Neurological Sciences 2007;260:33–7.

Journal of the Neurological Sciences 331 (2013) 76–80

Contents lists available at SciVerse ScienceDirect

Journal of the Neurological Sciences

journal homepage: www.elsevier.com/locate/jns

Impulsive compulsive behaviors in Japanese Parkinson's disease patients and utility of the Japanese version of the Questionnaire for Impulsive–Compulsive Disorders in Parkinson's disease

Kenichiro Tanaka *, Kenji Wada-Isoe, Satoko Nakashita, Mikie Yamamoto, Kenji Nakashima

Division of Neurology, Department of Brain and Neurosciences, Faculty of Medicine, Tottori University, Japan

ARTICLE INFO

Article history:
Received 26 January 2013
Received in revised form 4 May 2013
Accepted 10 May 2013
Available online 2 June 2013

Keywords:
Pathological gambling
Compulsive sexual behavior
Compulsive buying
Compulsive eating
Punding
Dopamine dysregulation syndrome

ABSTRACT

Background: In order to evaluate impulsive compulsive behaviors (ICBs), such as pathological gambling, compulsive sexual behavior, compulsive buying, compulsive eating, punding, and dopamine dysregulation syndrome (DDS) in Japanese Parkinson's disease (PD) patients, we constructed a Japanese version of the Questionnaire for Impulsive–Compulsive Disorders in Parkinson's disease (J-QUIP) and evaluated the utility of the J-QUIP in Japanese PD patients.
Methods: J-QUIP was administered to 121 PD patients. Diagnoses of ICBs were made via interview of patients or their caregivers. Subsequently, in order to evaluate risk factors related to these conditions, we evaluated demographic and clinical characteristics, clinical features, and medications utilized.
Results: We were able to administer the J-QUIP to 118 of 121 PD patients (97.5%). Sensitivity and specificity of J-QUIP were similar to that reported for the original version of QUIP. In our study, the actual prevalence of each disorder diagnosed via interview was as follows: pathological gambling (6.5%), compulsive sexual behavior (3.2%), compulsive buying (3.2%), compulsive eating (3.2%), punding (6.5%), and DDS (2.2%). Significantly risk factors for these conditions were younger age ($p = 0.047$), earlier age of disease onset ($p = 0.015$), longer PD duration ($p = 0.001$), total levodopa equivalent dose ($p = 0.006$), and dosage of levodopa ($p = 0.019$).
Conclusions: We evaluated the prevalence of ICBs in Japanese PD patients along with factors associated with these behaviors via J-QUIP.

1. Introduction

Besides classical motor symptoms, patients with Parkinson's disease (PD) also experience non-motor symptoms. These non-motor symptoms affect quality-of-life, institutionalization, and healthcare costs. Certain behaviors associated with PD are produced by chronic treatment with dopaminergic medications. These behaviors are linked by their incentive- or reward-based and repetitive natures [1], and are termed impulsive compulsive behaviors (ICBs). These behaviors include pathological gambling, compulsive sexual behavior, compulsive buying, compulsive eating, punding, and dopamine dysregulation syndrome (DDS). DDS means compulsive medication use. Especially, pathological gambling, compulsive sexual behavior, compulsive buying, and compulsive eating are often called impulsive–compulsive disorders (ICDs) [2]. Although ICBs represent one of the non-motor symptoms of PD, they are not very well identified by patients or family caregivers and are frequently overlooked in the clinical setting. In addition, whereas the prevalence and the risk factors of these behaviors were estimated in recent reports, it has not fully considered. Recently, Weintraub et al. have reported the utility of the Questionnaire for Impulsive–Compulsive Disorders in Parkinson's disease (QUIP), a self-administered questionnaire for impulsive–compulsive disorders [2]. QUIP can also screen punding and DDS. Of note, QUIP was used in Malaysia [3]. In this study, we developed a Japanese version of QUIP (J-QUIP) and evaluated the usefulness of J-QUIP in Japanese PD patients. Furthermore, we estimated the prevalence and the risk factors of ICBs in Japanese PD patients.

2. Material and methods

2.1. Development of J-QUIP

We developed a Japanese version of QUIP, employing procedures accepted internationally [4]. After obtaining permission from the authors of the original version of QUIP to produce the J-QUIP, we translated the original version of QUIP into the Japanese language. Next, the Japanese-translated QUIP was re-translated into English

* Corresponding author at: Division of Neurology, Department of Brain and Neurosciences, Faculty of Medicine, Tottori University, 36-1 Nishi-cho, Yonago 683-8504, Japan. Tel.: +81 859 38 6757; fax: +81 859 38 6759.
E-mail address: ken0815@med.tottori-u.ac.jp (K. Tanaka).

0022-510X/$ – see front matter © 2013 Elsevier B.V. All rights reserved.
http://dx.doi.org/10.1016/j.jns.2013.05.013

by a person unassociated with the first translation. Finally, we asked the original authors whether this back-translated version preserved the same meanings as the original, and this ultimately resulted in the J-QUIP. Although the original version of QUIP included both a full version questionnaire and a short version questionnaire, we employed only the short version questionnaire since no differences exist in the test sensitivity between these two versions [2].

2.2. Subjects

The subjects for this study comprised 121 consecutive patients diagnosed with idiopathic PD in the Department of Neurology at Tottori University Hospital between April 2011 and December 2011. The clinical diagnosis of PD was based on the UK PD Society Brain Bank criteria [5]. Demographic and clinical characteristics are as follows: Age (70.5 ± 9.7 years), Sex (male: female = 56: 65), PD duration (9.9 ± 7.3 years), and Hoehn–Yahr scale (2.6 ± 0.9). We evaluated demographic and clinical characteristics of each group, such as sex, age, age of disease onset, PD duration, degree of severity of motor symptoms, non-motor symptoms (depression, apathy, sleep disturbance, excessive daytime sleepiness, REM sleep behavior disorder, restless leg syndrome, fatigue, orthostatic hypotension, constipation, visual hallucination, and olfactory dysfunction), medications (total levodopa equivalent dose (LEDs) [6], dopamine agonist-only LEDs, levodopa, pramipexole, ropinirole, selegiline, and amantadine), heart-mediastinum (H/M) ratio of ^{123}I-meta-iodobezylguanidine (MIBG) myocardial scintigraphy [7], and amount of activity in actigraphy [8]. We assessed motor symptoms by using the Hoehn–Yahr scale, and certain non-motor symptoms via questionnaires. The employed questionnaires included the Geriatric Depression Scale-15 (GDS-15) [9], the Apathy Scale (AS) [10], the Pittsburgh Sleep Quality Index (PSQI) [11], the Japanese version of the Epworth Sleepiness Scale (JESS) [12], the REM Sleep Behavior Disorder Screening Questionnaire (RBDSQ) [13], and the Parkinson Fatigue Scale (PFS) [14]. GDS-15 has been validated for the diagnosis of depression, with the cut-off point being 5/6. AS has also been validated for apathy, with the cutoff point being 15/16. The cutoff value for the PSQI for poor sleep was 5/6 points, for the JESS to assess excessive daytime sleepiness was 9/10 points, and for the RBDSQ to detect REM sleep behavior disorder was 5/6 points. In addition, PFS was used to evaluate fatigue, and the cutoff point was 3.3. Regarding restless leg syndrome, fatigue, orthostatic hypotension, constipation, visual hallucination, and olfactory dysfunction, we assessed it positive or negative.

2.3. Diagnosis of ICBs

After administration of J-QUIP, we interviewed the patients directly or by telephone to confirm whether the patient experienced abnormal behaviors related to ICBs. In case we were unable to gather sufficient information from the patient, we also interviewed their caregiver. We diagnosed pathological gambling, compulsive sexual behavior, compulsive buying, compulsive eating, punding and DDS according to various diagnostic criteria as listed in the review by Voon and Fox [1].

2.4. Data analysis

Data analysis was conducted with SPSS for Windows version 18 (Chicago, IL). The results are presented as mean ± standard deviation. Intergroup differences were analyzed using a Mann–Whitney *U* test. Categorical variances were examined using a χ^2 test. We used a level of 95% ($P < 0.05$) as the criterion for statistical significance.

This study was planned and conducted in accordance with the Declaration of Helsinki. The Ethics Committee of the Tottori University Faculty of Medicine approved the study prior to its implementation.

3. Results

3.1. Validation of J-QUIP and prevalence of ICBs

We were able to administer the J-QUIP to 118 of 121 PD patients (97.5%), almost all within 5 min. Three patients rejected the survey due to their severe cognitive impairment. Of the 118 PD patients, 93 patients were able to confirm whether they experienced symptoms of ICBs via interviewing directly or by telephone. 25 patients were not able to confirm because we couldn't contact them. So, we decided to turn these 93 patients into this study (Fig. 1).

The prevalence of QUIP positivity in our patients was as follows: pathological gambling (14.0%), compulsive sexual behavior (14.0%), compulsive buying (10.8%), compulsive eating (10.8%), punding (16.1%), and DDS (18.3%) (Fig. 1).

The actual prevalence of ICBs which is determined by interview for patients was indicated in below: pathological gambling (6.5%), compulsive sexual behavior (3.2%), compulsive buying (3.2%), compulsive eating (3.2%), punding (6.5%), and DDS (2.2%) (Fig. 1 and Table 1). Regarding DDS, DDS was highest QUIP positive, but only 2 of 17 PD patients actually experienced compulsive medication use. Overall, 21.5% of PD patients had a history of at least one ICB and 12.9% of PD patients had a history of at least one ICD. In addition, we detected 2 patients (2.2%) who concealed their ICBs (one is pathological gambling, the other is punding) from their caregiver's interview.

Based on these results, we validated the utility of J-QUIP. We calculated sensitivity, specificity, positive predictive value (PPV), and negative predictive value (NPV) for each behavior via diagnostic concordance rate between actual diagnosis and result of J-QUIP. These are shown in Table 2.

3.2. Risk factors for ICBs

We evaluated risk factors for actual ICBs diagnosed via interview.

Regarding demographic features, younger age ($p = 0.047$), earlier age of disease onset ($p = 0.015$), and longer PD duration ($p = 0.001$) were all related to ICBs. Gender was unrelated to these conditions (Table 3).

Regarding motor symptoms, Hoehn–Yahr scale scores were not related to ICBs. Regarding non-motor symptoms, none of the symptoms studied, including depression, apathy, sleep disturbances, excessive daytime sleepiness, REM sleep behavior disorder, restless leg syndrome, fatigue, orthostatic hypotension, constipation, visual hallucination, or olfactory dysfunction, were related to ICBs (Table 3).

Regarding dopamine replacement therapy as medications, LEDs ($p = 0.006$) and dosage of levodopa ($p = 0.019$) were related to the prevalence of ICBs. Mean dose of dopamine agonist-only LEDs in the PD patients with ICBs was higher than that in the PD patients without ICBs, but the difference did not reach statistical significance. Other medications, such as dosage of pramipexole, dosage of ropinirole, dosage of selegiline, or dosage of amantadine, were not related. The use of dopamine agonists (any one of pramipexole, ropinirole, cabergoline, bromocriptine, or pergolide) was not also statistically related to the presence of ICBs (Table 3).

4. Discussion

In this study, we created a Japanese version of QUIP, which represents a screening questionnaire for ICBs. We also evaluated the usefulness of this test since the sensitivity and specificity of J-QUIP share similar detection rates as the original version of QUIP (Table 2). Previously, the Japanese versions of BIS-11 (Barratt Impulsive Scale-11) [15], SOGS (South Oaks Pathological gambling Screen) [16], and MOCI (Maudsley Obsessional–Compulsive Inventory) [17] have been used for the screening of impulsivity in Japan. In addition, the MIDI (Minnesota Impulsive Disorders Interview) has been used in foreign countries although it has

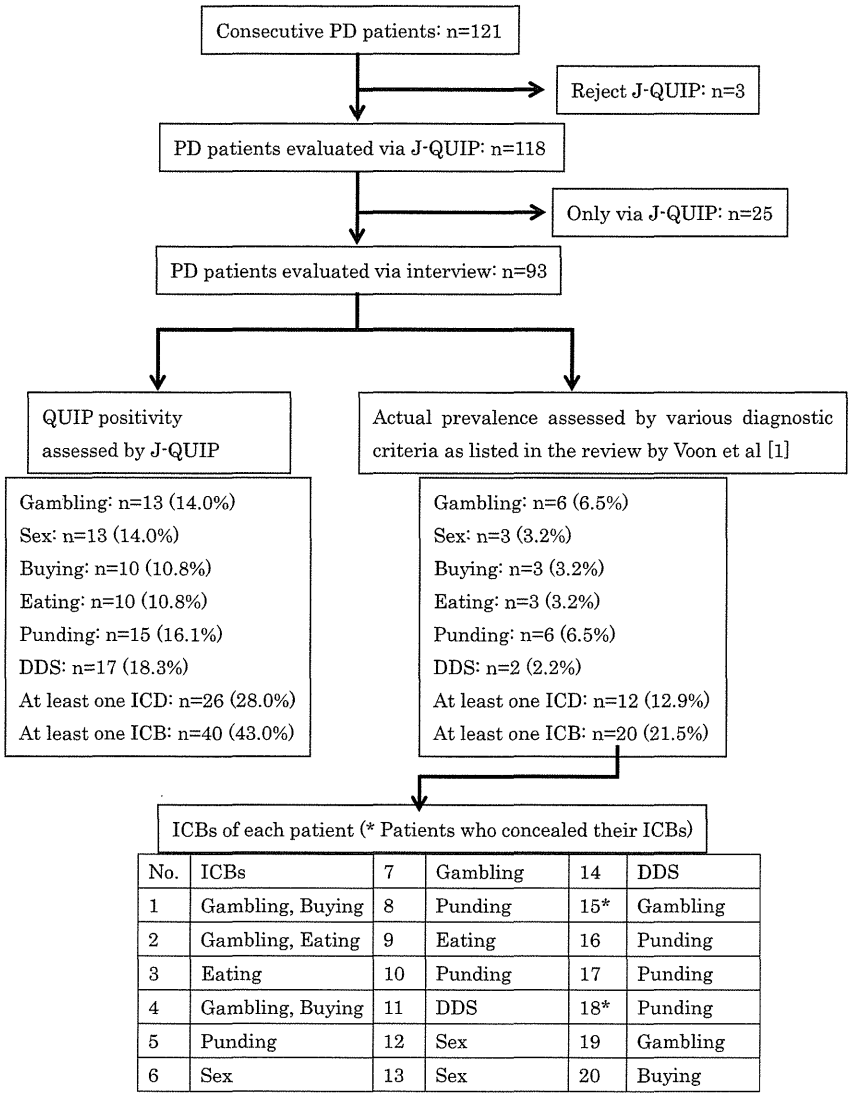

No.	ICBs	7	Gambling	14	DDS
1	Gambling, Buying	8	Punding	15*	Gambling
2	Gambling, Eating	9	Eating	16	Punding
3	Eating	10	Punding	17	Punding
4	Gambling, Buying	11	DDS	18*	Punding
5	Punding	12	Sex	19	Gambling
6	Sex	13	Sex	20	Buying

Fig. 1. Diagnostic flow chart for this study.

not been employed in Japan to our knowledge. However, these questionnaires assess limited symptoms and do not assess all types of ICBs, and these questionnaires were not developed specifically for PD. In contrast, QUIP can evaluate a comprehensive range of ICBs, such as pathological gambling, compulsive sexual behavior, compulsive buying, compulsive eating, punding, and DDS. Furthermore, QUIP was designed for PD patients. Therefore, it is likely that QUIP represents the most suitable questionnaire for PD patients in evaluating their ICBs.

Table 1
Prevalence of symptoms.

Report	Area	Gambling	Sex	Buying	Eating	ICDs	Punding	DDS	ICBs
Several authors [18]	Western	1.7~ 6.1%	2.0~ 10.0%	0.4~ 5.7%	2.4~ 4.3%	6.1~ 13.6%	1.4~ 14.0%	3.4~ 4.3%	–
Weintraub D et al. [19]	Western	5.0%	3.5%	5.7%	4.3%	13.6%	–	–	–
Lee JY et al. [20]	Korea	1.3%	2.8%	2.5%	3.4%	10.1%	4.2%	–	–
Chiang HL et al. [18]	Taiwan	1.49%	2.99%	0.00%	0.37%	4.48%	0.37%	1.12%	–
Fan W et al. [21]	China	0.32%	1.92%	0.00%	0.32%	3.21%	–	0.64%	–
[a]Lim SY et al. [3]	Malaysia	2.6%	8.2%	3.6%	8.7%	15.4%	13.8%	2.0%	24.6%
Present study	Japan	6.5%	3.2%	3.2%	3.2%	12.9%	6.5%	2.2%	21.5%

Gambling = pathological gambling, Sex = compulsive sexual behavior.
Buying = compulsive buying, Eating = compulsive eating.
[a] QUIP positivity (results from assessment only by QUIP).

Table 2
Validation of the J-QUIP.

		Gambling	Sex	Buying	Eating	Punding	DDS
Weintraub et al. study [2]	Sensitivity	91%	95%	80%	86%	63%	–
	Specificity	95%	90%	91%	85%	93%	–
	PPV	59%	48%	38%	21%	50%	–
	NPV	99%	100%	99%	99%	96%	–
Present study	Sensitivity	83.3%	100%	100%	100%	83.3%	100%
	Specificity	90.6%	100%	92.0%	92.0%	88.2%	81.7%
	PPV	38.5%	100%	30.0%	30.0%	33.3%	11.8%
	NPV	98.7%	100%	100%	100%	98.7%	100%

Gambling = pathological gambling, Sex = compulsive sexual behavior.
Buying = compulsive buying, Eating = compulsive eating.

The sensitivity and specificity for each ICB for J-QUIP were all over 80%, while NPVs for each ICB were close to 100%, demonstrating the utility of J-QUIP as a screening questionnaire in daily practice. J-QUIP is also a rapid screening questionnaire as it takes only 5 min to complete. However, it is necessary to interview patients who are screened as positive (in order to confirm the diagnosis of ICBs) because of the low PPVs and high false-positive rates for ICBs. If patients are screened as being negative, it strongly suggests that they do not have a history of ICBs. Furthermore, we need to note that some patients are screened as negative because they may conceal their symptoms. If symptoms are concealed, they are not detectable by the questionnaire. Indeed, at least 2 patients (2.2%) concealed their symptoms in our study.

The prevalence of ICBs in PD patients has also been reported in areas outside of Japan (Table 1). The prevalence of ICBs in our Japanese PD patients is similar to those reported in Western countries [18], although the prevalence was greater than that reported for other Asian countries, particularly Taiwan and China [18,21]. Although the reasons for these differences in prevalence are unclear, the frequency of using dopamine agonist therapy might account for the differences. Several studies have revealed that treatment with dopamine agonists is associated with the development of ICBs in PD patients [22,23,24,25]. The frequency of dopamine agonist utilization is much less in Taiwan and China than in Japan, Korea, or Western countries [21]. The prevalence of ICBs in Korean PD patients was almost the same as that in our Japanese patients, while only the prevalence of pathological gambling in Korean patients was much less compared to our Japanese patients [20]. In addition, the prevalence of pathological gambling in Japanese patients was somewhat higher than observed in Western patients. Pachinko (pinball) was reported to be the most prevalent avenue for pathological gambling in Japan [26]. In this study, almost all patients who experienced pathological gambling also played Pachinko. Thus, one possible reason why the prevalence of pathological gambling is high in Japanese PD patients is that it is influenced not only by medication, but also by environmental factors including easy access to Pachinko.

Previous studies have indicated that numerous factors including young age, early age of disease onset, longer duration of disease, dopamine agonist medications, pramipexole use, amantadine use, LEDs, and dosage of levodopa are related to ICBs in PD [22,23,24,25,27,28]. In our study, younger age, earlier age of disease onset and longer PD duration were related to ICBs. In addition, LEDs and dosage of levodopa were related to ICBs. Regarding dopamine agonist therapies, there were no significant differences in the frequency of dopamine agonist use between PD patients with ICBs and those without, but dopamine agonist-only LEDs ($p = 0.057$) might have some part of relation with ICBs. Regarding non-motor symptoms, depression was found to be associated with ICBs in PD [24,27,28], although relationships with non-motor symptoms are less reported than relationships with demographic factors and medications. In our study, no non-motor symptoms were related to control and repetitive behaviors. So, it seems likely that non-motor symptoms have little to no association with ICBs.

There are a few limitations of the current study to note. First, since we diagnosed ICBs based on interviews of patients and their caregivers, we might have overlooked symptoms when the patients failed to disclose

Table 3
Factors related to ICBs.

	Overall	ICBs group	Non-ICBs group	Statistical value
Demographic factors	n = 93	n = 20	n = 73	
Male:Female	46:47	12:8	34:39	p = 0.322*
Age (years)	69.3 ± 9.8	66.3 ± 7.6	70.2 ± 10.1	p = 0.047
Age of disease onset (years)	59.7 ± 11.9	53.0 ± 9.2	61.5 ± 11.9	p = 0.015
PD duration (year)	9.6 ± 6.6	12.9 ± 8.3	8.7 ± 5.9	p = 0.001
Motor, non-motor symptoms				
Hoehn–Yahr scale	2.6 ± 0.9	2.6 ± 0.8	2.6 ± 0.9	p = 0.851
MIBG (early image)	1.67 ± 0.39	1.61 ± 0.32	1.69 ± 0.40	p = 0.393
MIBG (late image)	1.50 ± 0.42	1.47 ± 0.40	1.51 ± 0.42	p = 0.615
Actigraphy	263 ± 190	216 ± 167	284 ± 200	p = 0.164
Depression(n)	60(65%)	11(55%)	49(67%)	p = 0.802*
Apathy(n)	58(62%)	9(45%)	49(67%)	p = 0.116*
Sleep disturbance(n)	49(53%)	14(70%)	35(48%)	p = 0.128*
Excessive daytime sleepiness(n)	30(32%)	9(45%)	21(29%)	p = 0.186*
REM sleep behavior disorder(n)	36(39%)	11(55%)	25(34%)	p = 0.121*
Restless leg syndrome(n)	14(15%)	4(20%)	10(14%)	p = 0.491*
Fatigue(n)	49(53%)	14(70%)	35(48%)	p = 0.130*
Orthostatic hypotension(n)	42(45%)	11(55%)	31(42%)	p = 0.447*
Constipation(n)	70(75%)	15(75%)	55(75%)	p = 1.000*
Visual hallucination(n)	25(27%)	6(30%)	19(26%)	p = 0.778*
Olfactory dysfunction(n)	34(37%)	9(45%)	25(34%)	p = 0.436*
Medication				
LEDs	554 ± 470	676 ± 325	520 ± 499	p = 0.006
Dosage of levodopa (mg)	374 ± 379	412 ± 145	366 ± 421	p = 0.019
Dosage of pramipexole (mg)	0.57 ± 1.13	1.10 ± 1.56	0.43 ± 0.94	p = 0.121
Dosage of ropinirole (mg)	1.40 ± 3.18	1.45 ± 3.14	1.39 ± 3.22	p = 0.860
Dosage of selegiline (mg)	1.48 ± 2.13	2.00 ± 2.76	1.33 ± 1.91	p = 0.402
Dosage of amantadine (mg)	18.8 ± 56.6	20.0 ± 54.8	18.5 ± 57.4	p = 0.865
Dopamine agonist-only LEDs	86.4 ± 119.2	139 ± 147	71.6 ± 106.8	p = 0.057
Taking dopamine agonist(n)	52(56%)	13(65%)	39(53%)	p = 0.449*

Mann–Whitney *U* test.
* χ^2 test

them and/or if their caregivers took no notice of them. Therefore, the prevalence in our study may represent a minimum, and it is possible that the actual prevalence was higher than that reported. Second, we could not conduct a multivariate analysis with respect to each ICB due to the small number of patients. Finally, since our study population was only PD patients who were able to visit our hospital, we did not study a true random sample of PD patients.

In conclusion, we verified the usefulness of the J-QUIP as a screening questionnaire for ICBs, and report that the prevalence of ICBs in Japanese PD patients appears to be similar to that reported in patients in Western countries. In addition, some demographic factors as well as medications were associated with the prevalence of ICBs in our study.

Conflict of interest

We have no conflict of interest.

Acknowledgments

We thank Weindraub D for the permission of use QUIP and the staff at the Department of Neurology at Tottori University for their help in recruiting the patients. This work was supported by Grants-in-Aid from the Research Committee of CNS Degenerative Disease, the Ministry of Health, Labour and Welfare of Japan.

References

[1] Voon V, Fox SH. Medication-related ICBs in Parkinson's disease. Arch Neurol 2007;64:1089–96.
[2] Weintraub D, Hoops S, Shea JA, Lyons KE, Pahwa R, Driver-Dunckley ED, et al. Validation of the questionnaire for impulsive–compulsive disorders in Parkinson's disease. Mov Disord 2009;24:1461–7.
[3] Lim SY, Tan ZK, Ngam PI, Lor TL, Mohamed H, Schee JP, et al. Impulsive–compulsive behaviors are common in Asian Parkinson's disease patients: assessment using QUIP. Parkinsonism Relat Disord 2011;17:761–4.
[4] Guillemin F, Bombardier C, Beaton D. Cross-cultural adaptation of health-related quality of life measures: literature review and proposed guidelines. J Clin Epidemiol 1993;46:1417–32.
[5] Gibb WR, Lees AJ. The relevance of the Lewy body to the pathogenesis of idiopathic Parkinson's disease. J Neurol Neurosurg Psychiatry 1988;51:745–52.
[6] Claire L, Stowe R, Patel S, Rick C, Gray R, Clarke CE. Systematic review of L-dopa dose equivalency reporting in Parkinson's disease. Mov Disord 2010;15:2649–53.
[7] Wada-Isoe K, Kitayama M, Nakaso K, Nakashima K. Diagnostic markers for diagnosing dementia with Lewy bodies: CSF and MIBG cardiac scintigraphy study. J Neurol Sci 2007;260:33–7.
[8] Uemura Y, Wada-Isoe K, Nakashita S, Nakashima K. Mild parkinsonian sign in a community-dwelling elderly population sample in Japan. J Neurol Sci 2011;304:61–6.
[9] Niino N, Imaizumi T, Kawakami N. A Japanese translation of the geriatric depression scale. Clin Gerontol 1991;10:85–6.
[10] Okada K, Kobayashi S, Aoki K, Suyama N, Yamaguchi S. Assessment of motivational loss in poststroke patients using the Japanese version of Starkstein's apathy scale. Jpn J Stroke 1998;20:318–23.
[11] Buysse DJ, Reynold III CF, Monk TH, Berman SR, Kupfer DJ. The Pittsburgh sleep quality index: a new instrument for psychiatric practice and research. Psychiatry 2003;18:498–505.
[12] Takegami M, Sugimoto Y, Wakita T, Noguchi H, Chin K, Kadotani H, et al. Development of a Japanese version of the Epworth sleepiness scale (JESS) based on item response theory. Sleep Med 2009;10:556–65.
[13] Stiasny-Kolster K, Mayer G, Schäfer S, Möller JC, Heinzel-Gutenbrunner M, Oertel WH. The REM sleep behavior disorder screening questionnaire — a new diagnostic instrument. Mov Disord 2007;22:2386–93.
[14] Brawn RG, Dittner A, Findley L, Wessely SC. The Parkinson fatigue scale. Parkinsonism Relat Disord 2005;11:49–55.
[15] Someya T, Sakado K, Seki T, Kojima M, Reist C, Tang SW, et al. The Japanese version of the Barratt impulsiveness scale, 11th version (BIS-11): its reliability and validity. Psychiatry Clin Neurosci 2001;55:111–4.
[16] Kido M, Shimazaki T. Reliability and validity of the modified Japanese version of the South Oaks pathological gambling screen (SOGS). Shinrigaku Kenkyu 2007;77:547–52.
[17] Tadai T, Nakamura M, Okazaki S, Nakajima T. The prevalence of obsessive–compulsive disorder in Japan: a study of students using the Maudsley Obsessional–Compulsive Inventory and DSM-III-R. Psychiatry Clin Neurosci 1995;49:39–41.
[18] Chiang HL, Huang YS, Chen ST, Wu YR. Are there ethnic difference in impulsive/compulsive behaviors in Parkinson's disease? Eur J Neurol 2012;3:494–500.
[19] Weintraub D, Koester J, Potenza MN, Siderowf AD, Stacy M, Voon V, et al. Impulse control disorders in Parkinson disease: cross-sectional study of 3090 patients. Arch Neurol 2010;67:589–95.
[20] Lee JY, Kim JM, Kim JW, Cho J, Lee WY, Kim HJ, et al. Association between the dose of dopaminergic medication and the behavioral disturbances in Parkinson disease. Parkinsonism Relat Disord 2010;16:202–7.
[21] Fan W, Ding H, Ma J, Chan P. Impulse control disorders in Parkinson's disease in a Chinese population. Neurosci Lett 2009;465:6–9.
[22] Weintraub D, Siderowf AD, Potenza MN, Goveas J, Morales KH, Duda JE, et al. Association of dopamine agonist use with impulse control disorders in Parkinson disease. Arch Neurol 2006;63:969–73.
[23] Voon V, Hassan K, Zurowski M, de Souza M, Thomsen T, Fox S, et al. Prevalence of repetitive and reward-seeking behaviors in Parkinson disease. Neurology 2006;67:1254–7.
[24] Pontone G, Williams JR, Bassett SS, Marsh L. Clinical features associated with impulse control disorders in Parkinson disease. Neurology 2006;67:1258–61.
[25] Evans AH, Strafella AP, Weintraub D, Stacy M. Impulsive and compulsive behaviors in Parkinson's disease. Mov Disord 2009;24:1561–70.
[26] Fujimoto K. Disinhibitory abnormal behavior induced by treatment of Parkinson disease. Brain Nerve 2012;64:373–83.
[27] Evans AH, Lawrence AD, Potts J, Appel S, Lees AJ. Factors influencing susceptibility to compulsive dopaminergic drug use in Parkinson disease. Neurology 2005;65:1570–4.
[28] Evans AH, Katzenschlager R, Paviour D, O'Sullivan JD, Appel S, Lawrence AD, et al. Punding in Parkinson's disease: its relation to the dopamine dysregulation syndrome. Mov Disord 2004;19:397–405.